1993

Detailed stratigraphic correlation of the Neogene sedimentary sequences on the Ontong Java Plateau by well logging; ODP Sites 803, 805, 806, 807, and DSDP Site 586

Mitchell Lyle
Borehole Research Group

Roy H. Wilkens
University of Hawaii - West Oahu

Larry A. Mayer
University of New Hampshire, larry.mayer@unh.edu

Berger, W.H., Kroenke, L.W., Mayer, L.A., et al., 1993
Proceedings of the Ocean Drilling Program, Scientific Results, Vol. 130

35. DETAILED STRATIGRAPHIC CORRELATION OF THE NEOGENE SEDIMENTARY SEQUENCES ON THE ONTONG JAVA PLATEAU BY WELL LOGGING: ODP SITES 803, 805, 806, 807, AND DSDP SITE 586[1]

Mitchell Lyle,[2] Roy H. Wilkens,[3] and Larry A. Mayer[4]

ABSTRACT

We used well logs, in some cases combined with shipboard physical properties measurements to make more complete profiles and to correlate between sites on the Ontong Java Plateau. By comparing sediment bulk density, velocity, and resistivity logs from adjacent holes at the same site, we showed that even subtle features of the well logs are reproducible and are caused by variations in sedimentation. With only minor amounts of biostratigraphic information, we could readily correlate these sedimentary features across the entire top of the Ontong Java Plateau, demonstrating that for most of the Neogene the top of the plateau is a single sedimentary province. We found it more difficult, but still possible, to correlate in detail sites from the top of the plateau to those drilled on the flanks. The pattern of sedimentation rate variation down the flank of the plateau cannot be interpreted as simply controlled by dissolution. Site 805, in particular, oscillates between accumulating sediment at roughly the same rate as cores on top of the Ontong Java Plateau, and accumulating sediment as slowly as Site 803, 200 m deeper in the water column. These oscillations do not match earlier reconstructions of central Pacific carbonate compensation depth variations.

INTRODUCTION

The sediments of the Ontong Java Plateau potentially contain a detailed record of the Neogene evolution of the western equatorial Pacific Ocean, provided that one can separate local variations in sedimentation from regional features related to paleoceanographic change. In this paper, we will examine the changes in sedimentation at drill sites across the top of the Ontong Java Plateau and down its eastern flank (Fig. 1) to search for regionally coherent patterns of sedimentation and to discover whether it is possible to observe and refine the Neogene changes in the carbonate compensation depth (CCD) reported for the central equatorial Pacific Ocean (Berger, 1973; van Andel et al., 1975). Because all of the sites are from above the actual CCD, we hoped to monitor CCD changes by the dissolution pattern at sublysocline drill sites. By comparing sediment accumulation for equivalent intervals, we hoped to monitor dissolution down the flank of the plateau.

Stratigraphic correlation is the basis for any paleoceanographic study involving more than one sediment core or Ocean Drilling Program (ODP) drill site. For reasonably complete ODP sections, the stratigraphic control of choice is the oxygen isotopic record of benthic foraminifers, because it is well known that this signal is synchronous within about a 1000 yr throughout the oceans and because the measurement of oxygen isotopes on foraminifers has become routine (Shackleton et al., 1984; Imbrie et al., 1984; Martinson et al., 1987). This correlation method has its drawbacks, however, in older sediments and for thick sedimentary sequences. First of all, a complete stratigraphic record is dependent upon core recovery. When the sediments become lithified and core recovery drops, difficulties quickly arise in assigning specific oxygen isotope excursions to the master stratigraphic record. For thick sedimentary sequences, too, it takes too long and costs too much to measure oxygen isotopes in the detail needed for stratigraphic purposes.

For these reasons, we decided to investigate whether well logs could be used for stratigraphic control for high-resolution paleoceanographic studies. Well logs have the advantage that the data is continuously recorded and are available at sea where they potentially can be used by shipboard scientists during drilling operations and in the initial interpretation of the sediment section. The data are of the best quality in the lithified sections where core recovery begins to drop and where continuous composite sections cannot be reconstructed from recovered core. And, by recording a variety of physical and chemical properties of the sediments, the ODP well logging program provides multiple potential stratigraphic tools.

The sediments of the Ontong Java Plateau provide a good test of the use of well logs for high-resolution stratigraphy. The Neogene sediment column everywhere on the plateau is a monotonous sequence of pelagic carbonate oozes (Kroenke, Berger, Janecek, et al., 1991). Only subtle variations in physical properties were noted in the cores, except for diagenetic cementation. Although no distinct sedimentary layers can be used for correlation, the biostratigraphy is excellent (Kroenke, Berger, Janecek, et al., 1991). Sedimentary layers on the plateau should have major lateral extent because the Ontong Java Plateau has always been pelagic (Resig et al., 1976) and because the plateau has always been under the open ocean. The continuity of sedimentary layers is indicated by seismic reflection records across the plateau (Mayer et al., 1991). Acoustic reflectors can be correlated easily from one side of the Ontong Java Plateau to the other. Well logs, with their better resolution than seismic reflection, should prove to be even more useful for stratigraphic correlation.

Our strategy, in this paper, is to first demonstrate the reproducibility of well log data by comparing logs of duplicate sections in Holes 807A and 807C. Then, when we have established the precision with which well log data can be recorded, we will use an inverse correlation technique (Martinson et al., 1987) to map each site to the standard Neogene stratigraphic section, represented by the section from Hole 806B. In addition, the Paleogene/Neogene sections recovered in Sites 807 and 803 will be correlated to each other. After we have correlated the sections, we will discuss the paleoceanographic implications and use a crude time scale to investigate the periodicities in our records.

All well logs used in this paper were recorded by Schlumberger, using their standard logging tools. A description of the tools used and

[1] Berger, W.H., Kroenke, L.W., Mayer, L.A., et al., 1993. *Proc. ODP, Sci. Results,* 130: College Station, TX (Ocean Drilling Program).

[2] Borehole Research Group, Lamont-Doherty Geological Observatory, Columbia University, Palisades, NY 10964, U.S.A. (present address: 5840 Collister Drive, Boise, ID 83703, U.S.A.).

[3] Institute of Geophysics, School of Ocean and Earth Science and Technology, University of Hawaii, 2525 Correa Road, Honolulu, HI 96822, U.S.A.

[4] Ocean Mapping Group, Department of Surveying and Engineering, University of New Brunswick, P.O. Box 4400, Fredericton, New Brunswick, E3B 5A3 Canada.

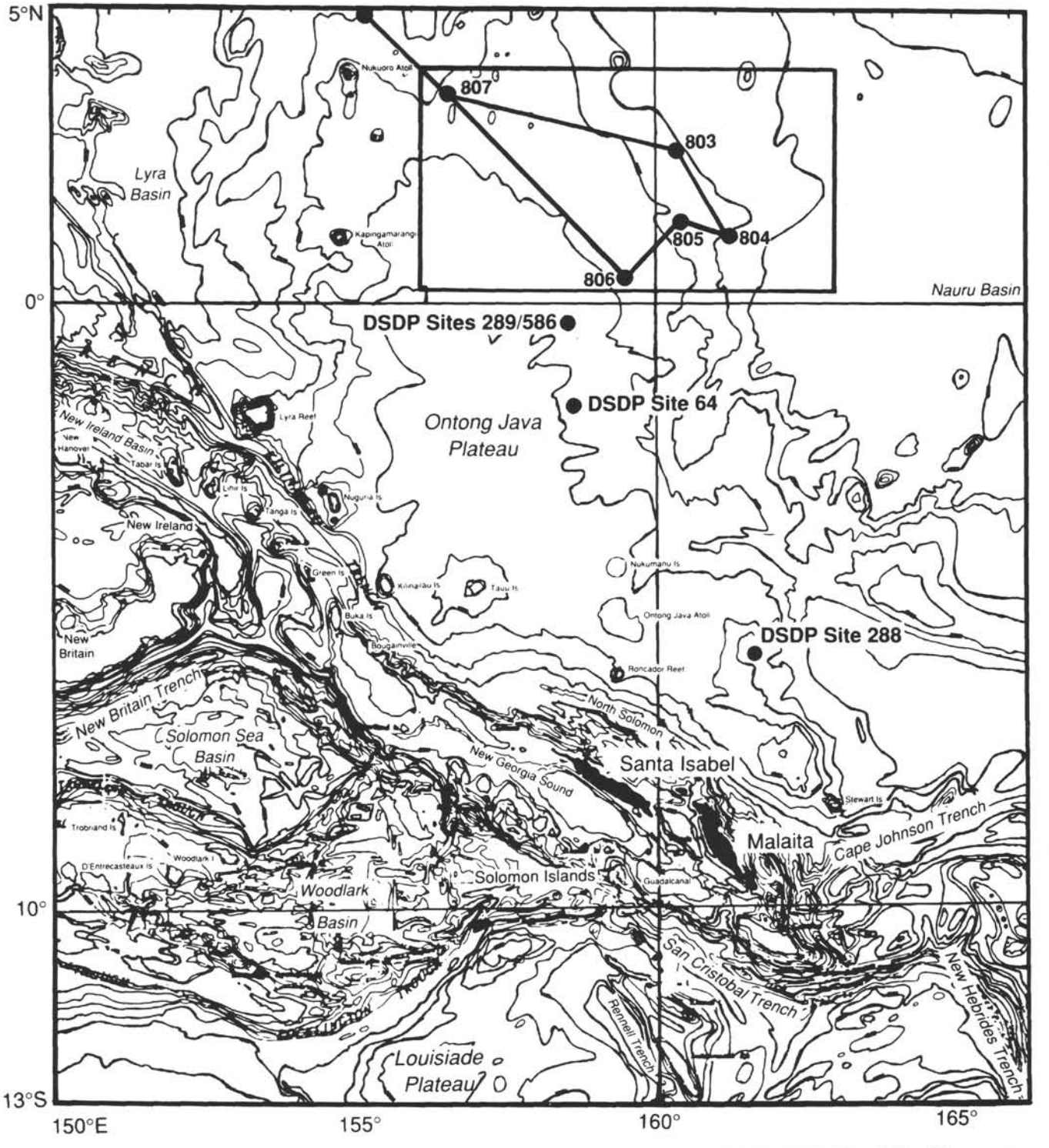

Figure 1. Bathymetry of the Ontong Java Plateau showing the locations of the drill sites on ODP Leg 130 (803–807) and DSDP Leg 89 Site 586.

the operational conditions in each hole are given in Kroenke, Berger, Janecek, et al. (1991). In general, hole conditions and the depth at which we set pipe for the logging runs prevented the use of logging data for the correlation of Pliocene-Pleistocene sections. Good correlations from the logs begin before about 5 Ma (latest Miocene) and continue back in time until diagenetic cherts become common in the section, in the Eocene.

CORRELATION OF HOLES 807A AND 807C

The physical properties variations we measured on the Ontong Java Plateau with well logs are subtle, and for this reason we wanted to confirm their reproducibility. Figure 2 illustrates the level of variation for the shallow focused resistivity log (SFLU), played back at a standard scale used in the oil industry. Note how the entire

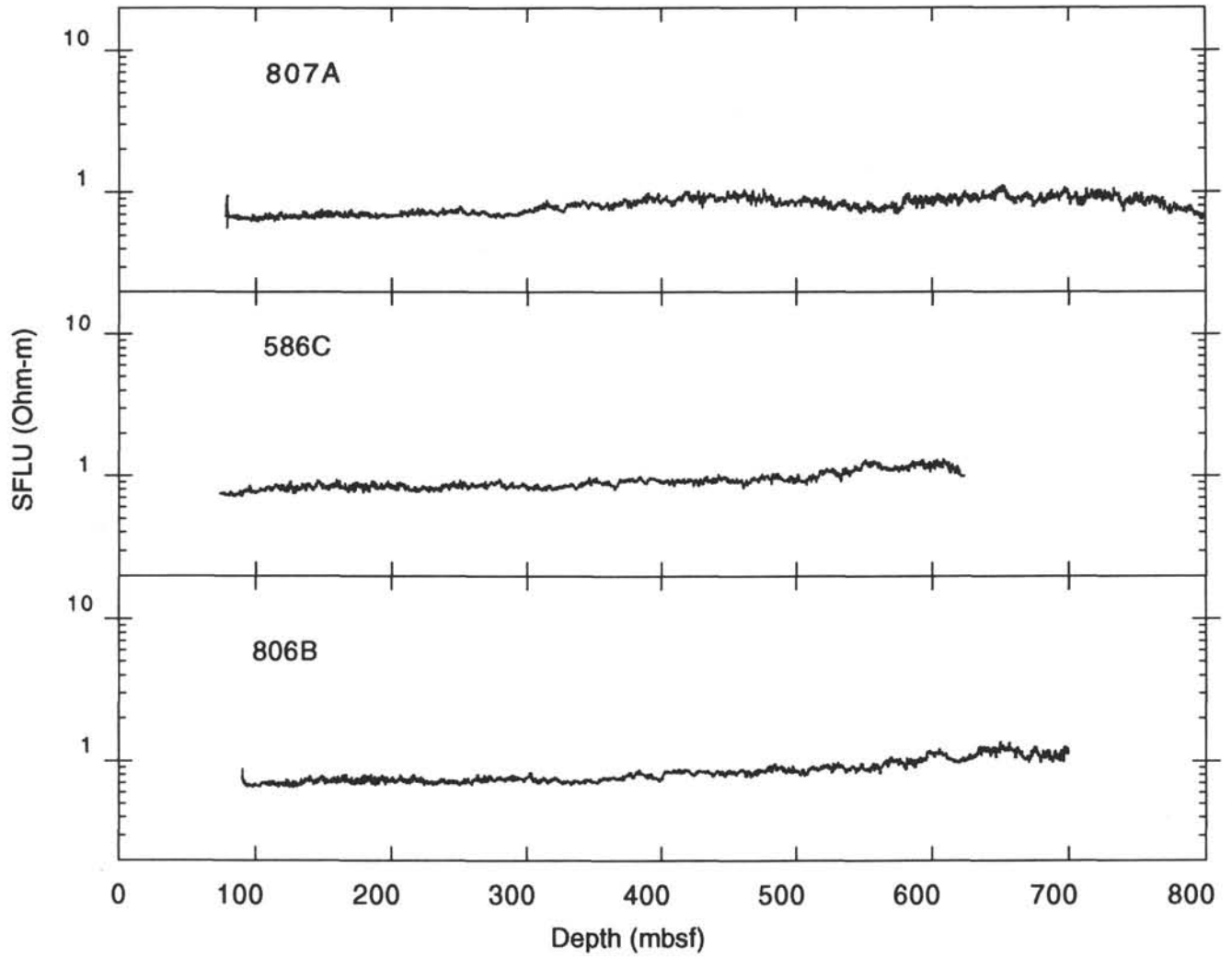

Figure 2. The shallow-focused resistivity logs for the three sites on top of the Ontong Java Plateau at a scale typically used to display ODP logs. The figure illustrates how small are the variations in the Neogene ooze and chalk sequence. For logs to be useful for paleoceanography, even these small variations must be reproducible.

Neogene section has only minor resistivity changes (the Miocene/Oligocene boundary is at about 740 mbsf in Hole 806B, at 590 mbsf in Hole 807A, and would be at about 700 mbsf at Site 586). For such variations to be useful for stratigraphy, they must be reproducible.

Hole 807A is the pilot hole drilled at Site 807, in a water depth of 2803.8 m. It was with the advanced hydraulic piston corer (APC) and the extended core barrel (XCB) to 822.9 mbsf and logged with the standard logging suite from 820 mbsf to the end of pipe at 85.6 mbsf. Hole 807C was drilled about 100 m north of Hole 807A, for a reentry hole to basement and was cased to 350 mbsf. Nevertheless, we were able to log in Hole 807C between 350 and 820 mbsf a section equivalent to the one in Hole 807A. The two holes provide a means to test the level to which hole conditions and tool response limit our ability to correlate between holes by means of logs.

With only minor depth shifting, discussed in more detail later, we can get excellent reproducibility between the logs from the two holes (Fig. 3). The worst disagreement occurs with the shallow focused resistivity log in the interval above 520 mbsf; this is caused by uncorrected borehole size effects in the log data. These types of effects shift the baseline resistivity values but still leave the high-frequency variations intact. We can examine the scale of variation by comparing the Hole 807A logs to the Hole 807C logs in a typical interval, between 550 and 600 mbsf. In each case, although slight baseline offsets may be present, we find that the residual standard deviations are <0.02 ohm-m for SFLU, <0.02 g/cm^3 for wet-bulk density, and <0.02 km/s for sonic velocity.

CORRELATION OF ALL ONTONG JAVA PLATEAU SITES

We used the SFLU shallow resistivity log to correlate the drill sites on top of the Ontong Java Plateau (806, 807, and 586) because this log has the highest frequency response of any of the logs we recorded on each hole. For sites down the margin of the plateau (803 and 805), we found that the bulk density logs are significantly more coherent with logs from sites on top of the Ontong Java Plateau than the SFLU, as we will discuss later. We used an inverse signal correlation technique, described in Martinson et al. (1982) and available as a computer package (CORPAC), to correlate among the drill sites. Briefly, the technique involves comparing a "distorted" time or depth series to a reference record and recovering a mapping function that makes the two similar. The aim of the inverse technique is to maximize

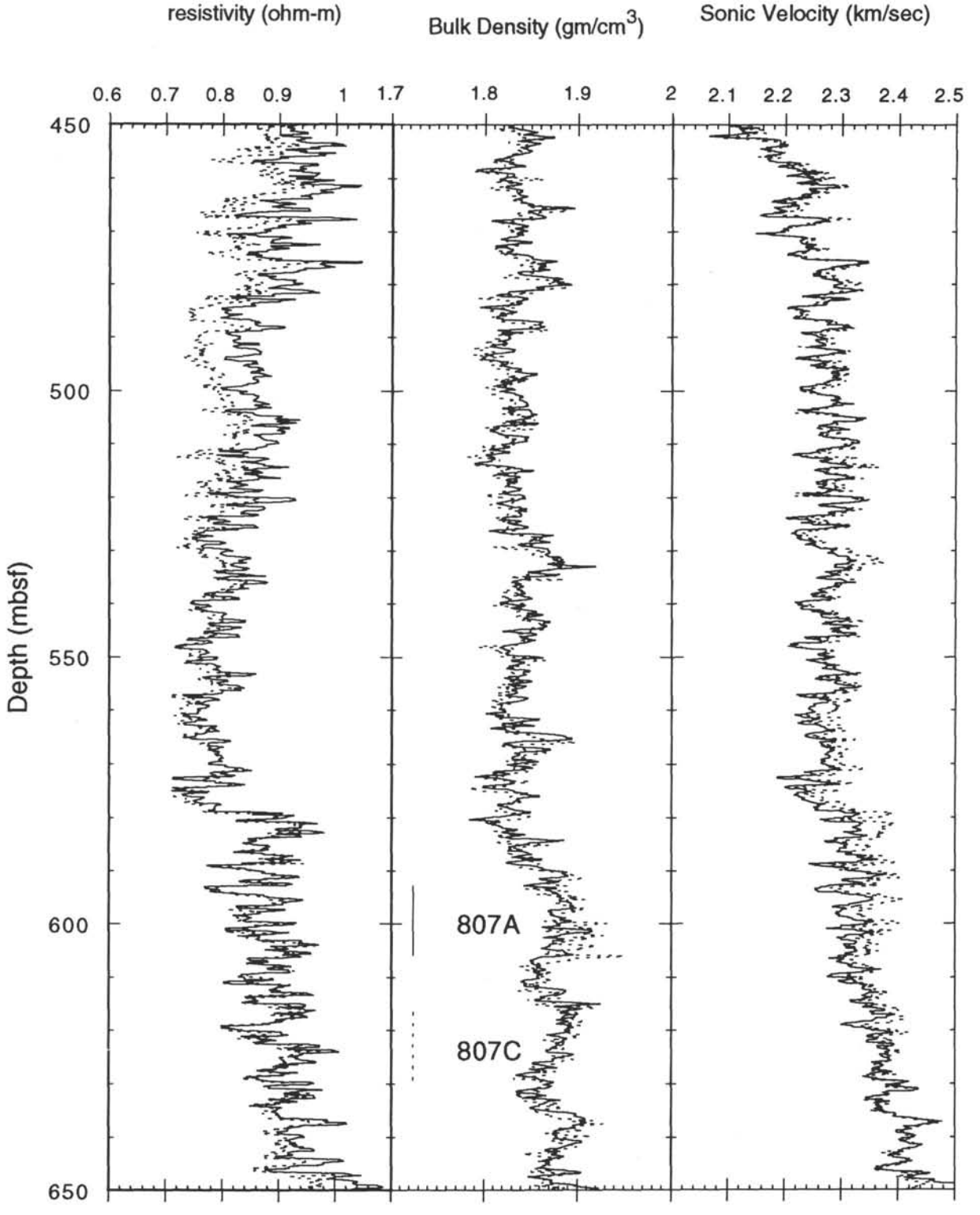

Figure 3. A comparison of logging data between Holes 807A and 807C, 100 yards apart. The data were depth shifted by the inversion technique described in the paper to remove the effects of minor sedimentation rate variations between the two holes. Sonic velocity (km/sec) is from the near-spaced sensors; wet bulk density in gm/cm^3; resistivity, from the shallow focused resistivity log (ohm-m).

coherence between the two normalized time series by assuming that the mapping function is a combination of linear and harmonic distortions. It iterates from an initial guess along the gradient of maximum coherence increase per change in the harmonic coefficients until coherence is maximized. The computer package is also interactive. We used a few biostratigraphic tie-points between holes as the initial guess for the correlation and graphically compared the resulting computer-generated correlation. We used this comparison to redefine the tie-points and repeat the process. Afterward, we compared this correlation to the other independent biostratigraphic information.

The Ontong Java Plateau Top: Sites 806, 586, and 807

The three sites on top of the Ontong Java Plateau—Site 806 (00°19.11′N, 159°21.66′E, 2520 m water depth), DSDP Site 586 (00°29.84′S, 158°29.89′E, 2208 m water depth), and Site 807 (3°36.36′N, 156°37.5′E, 2804 m water depth)—demonstrate the facility with which holes can be correlated under ideal conditions. The quality of the correlation also shows that the sediments at each of the sites on top of the Ontong Java Plateau contain a record of regional paleoceanographic events and not local sedimentary accidents.

At each site, we used the drill string "bottom felt" data to convert from meters below the rig floor to meters below seafloor. We subtracted 2531.0 m from the total wire out on the logging runs for Hole 806B as the depth to the seafloor; for Hole 807A we subtracted 2815.1 m; for Hole 807C we subtracted 2817.0 m; and for Hole 586C we subtracted 2218.0 m. We used Hole 806B as our reference hole because shipboard biostratigraphy had already shown that this drill site had the highest sedimentation rate and so its record has the highest stratigraphic resolution.

To get the initial stratigraphic ties for the CORPAC inverse signal correlation package, we normally used a few of the biostratigraphic datum levels as initial depth ties between cores. For Holes 807A and 807C, the biostratigraphic data was not needed as the holes are so close to each other and their sedimentation rates are almost the same. For the correlation of Hole 586C to Hole 806B, we used three nannofossil datum levels as initial tie-lines between the two cores: the last occurrence (LO) of *Ceratolithus acutus* (4.6 Ma), the LO of *Discoaster quinqueramus* (5.0 Ma), and the LO of *Discoaster hamatus* (8.7 Ma). We used two initial datum levels to tie Holes 807A and 806B: the LO of the foraminifer *Globorotalia kugleri* (20.9 Ma) and the LO of the nannofossil *Discoaster quinqueramus* (5.0 Ma).

Sites 806 and 807

The correlation between Holes 806B and 807A proved to be straightforward. Although we started by trying to correlate the SFLU shallow resistivity logs, we changed to correlating the medium penetration resistivity (IMPH) logs because the high resolution of the SFLU actually confused the correlation program. The sedimentation rate at Hole 807A was sufficiently slower at Hole 806B so that what appeared as one peak on the SFLU log at Hole 807A would be present as multiple peaks in Hole 806B. Nevertheless, we achieved a high-quality correlation between the two records (Fig. 4). The record above 520 mbsf (approximately 14.9 Ma) is easily matched between the two holes. Below this depth, however, the SFLU logs diverge from each other, as well as all other logs from the two drill sites. Figure 5 shows the velocity and SFLU logs for this interval. The velocity logs are offset from each other, because equivalent sedimentary ages are at different depths in the two cores, and sediment compaction adds a significant linear trend to the velocity data (Urmos et al., this volume). Except for the depth-related offset, small features above 520–550 mbsf can easily be correlated. Below this depth, the coherence between the two records is significantly smaller.

We were able to check our correlation by the independently determined biostratigraphic information (Fig. 6). The mapped correlation between Holes 807A and 806B connects the detailed nannofossil correlation scheme redone for this volume (Takayama and Backman, this volume). Thus, stratigraphy based upon the physical properties of the sediments at Sites 806 and 807 gives a correlation indistinguishable but in much more detail from the biostratigraphy in the two holes. The equivalent depths at Sites 807 and 806 can be found in Table 1.

Sites 806 and 586

The correlation between Holes 586C and 806B required little effort because the records almost perfectly match each other. We used the SFLU resistivity curves and were able to reach a coherence of 0.96 between the two logs with 19 harmonic coefficients (Fig. 7). Again the comparison to the biostratigraphy shows that this seems to be a reasonable correlation (Fig. 8). In this case, however, biostratigraphic information exists to only 300 mbsf in the hole because the lower 300 m was washed and not cored. The deepest biostratigraphic point shown in Figure 7, that of the last occurrence of *D. hamatus*, is somewhat off the log correlation line, but the Leg 89 biostratigraphers noted that they only tentatively reached this datum (Moberly, Schlanger, et al., 1986). *D. hamatus* was extremely rare in the last core catcher and could have been reworked. The correlation listed in Table 1 would put the actual last occurrence of *D. hamatus* to be about 17 m deeper at Site 586. Here again, where a reasonable likelihood exists that the sediments at each drill site are similar, we have found that we can correlate the two sites in detail.

Implications of the Correlation

All the SFLU records from the sites on top of the Ontong Java Plateau contain a record of basically the same signal with only minor variations (Fig. 9), at least from approximately 14.9 Ma to the top of our logging correlations, at 5 Ma. These sites are not adjacent to each other, but they span approximately 500 m in water depth and are as much as 485 km apart (Sites 807 and 806; see Fig. 1).

The relatively high frequency of the events implies that they should be driven by Milankovitch insolation cycles. Figure 10 shows a spectral analysis from a section between about 3.5 to 8.75 Ma (based on biostratigraphy) of the shallow resistivity log from Hole 806B. This particular interval was assumed to have a constant sedimentation rate of 45.8 m/m.y. The record contains spectral power at or about the 120, 95, 41, 23, and 19 k.y. Milankovitch periods. Because the higher frequency 41 and 23 k.y. peaks are split, however, we think that the original time scale is overly simplified and that the sedimentation rate is not completely constant in this interval. By producing evolutionary spectra for this interval, we will be able to identify where the sedimentation rate changes occur and revise the time scale.

The Milankovitch orbital variations in solar insolation have in some manner affected the electrical resistivity of the sediment column. Because sediment resistivity is most strongly affected by porosity, we think that we are observing small-scale, coherent porosity variations from every drill site on top of the Ontong Java Plateau. We are uncertain what could have caused porosity to vary, but it may represent a grain-size effect. If so, the porosity variations could represent changes in winnowing caused by average current speeds over the plateau or by the average strength of tidal flow. We wish to reiterate, however, that the quality of the correlations across the entire top of the Ontong Java Plateau implies that the environmental changes that caused variations in porosity must be regional in scale. Local current variations could not have caused the observed patterns.

Correlation of Plateau Flank Holes to Plateau Top Holes: Sites 803, 805, 806, and 807

Not surprisingly, the holes down the flank of the Ontong Java Plateau were more difficult to correlate to the reference drill site (Hole 806B) than holes from the top of the plateau. Because the

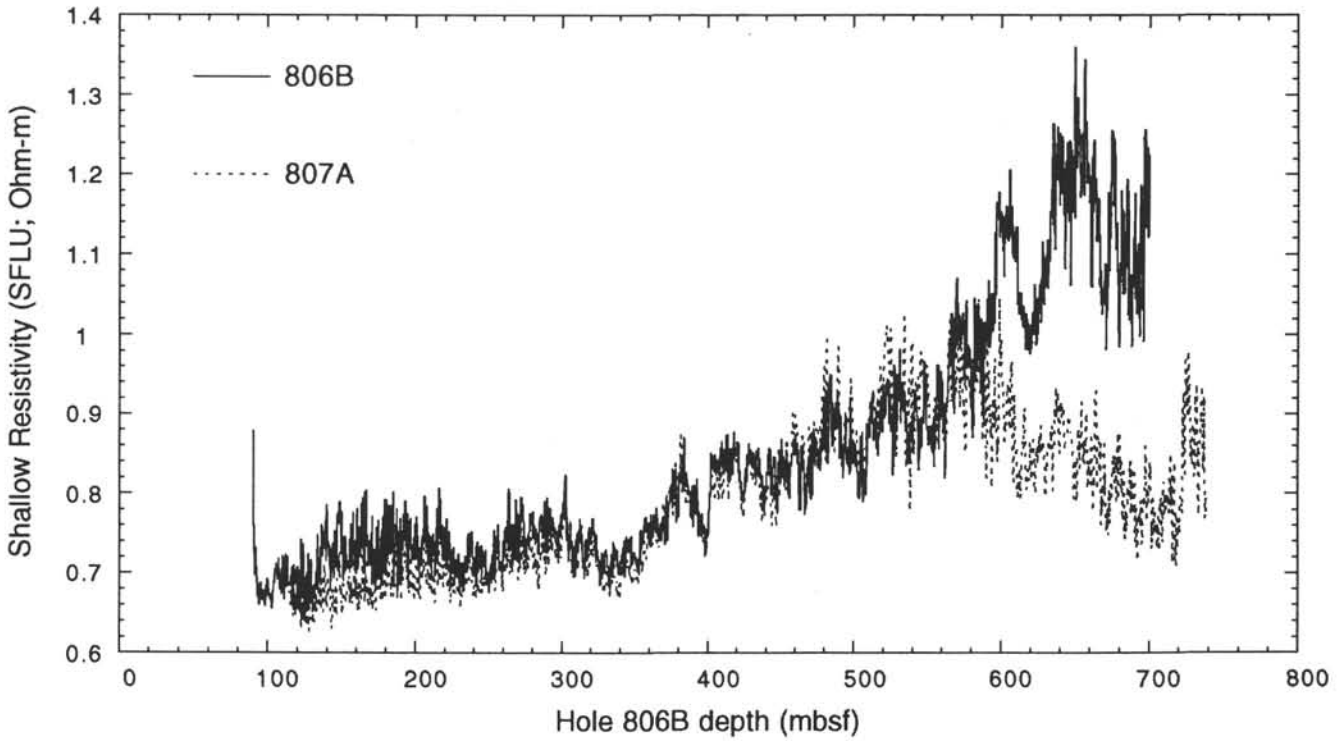

Figure 4. The SFLU shallow resistivity logs for Holes 806B and 807A, about 485 km apart, plotted on the correlation depth scale of Hole 806B. Note how the upper part of the holes have a very high coherence, but the lower Miocene sections diverge, below 550 mbsf.

attempted correlation is of sediment physical properties, changes in sedimentation regime, whether through dissolution or through changes in deposition style, will strongly affect the records. Sites 805 (1°13.7′N, 160°31.8′E, 3188 m water depth) and 803 (2°26.0′N, 160°32.5′E, 3412 m water depth) were cored as part of the depth transect down the flank of the plateau to examine water mass properties and to monitor fluctuations in carbonate dissolution with time. Site 804 (1°00.3′N, 161°35.6′E, 3862 m water depth) was not logged and will not be included in this report.

As explained below, we first attempted to correlate both sites to Site 806 by means of the resistivity records; however, we later decided that the bulk density logs contained more of a common signal. We also decided to correlate Site 803 to 807, because Site 806 had insufficient record length for a good correlation, and because we found systematic differences in the physical properties of the northern cores (Sites 803 and 807) and the southern ones (Sites 586, 806, and 805). We will discuss these systematic differences in more detail later. The correlation of Sites 803 and 806 was then achieved by means of the Site 807/806 correlation.

We found that correlations between Sites 806 and 805 based upon the SFLU resistivity suffered because of ambiguity in the logs from the deeper hole. The SFLU logs for the middle to late Miocene age section at Site 805 have about half the variance of Site 806, whereas the two bulk density logs are much more similar in amplitude. Thus, matching peaks is much easier when using bulk density logs. In the correlation of Sites 803 and 807, we found low coherence between the SFLU logs. The best coherence we could obtain by correlating the SFLU logs was 0.50 (1.0 is perfect coherence—i.e., an exact match between records), whereas we achieved a coherence of 0.87 by correlating the bulk density logs and matched the independent biostratigraphic data better.

For Sites 806 and 803, we used a combined data set of both discrete shipboard bulk density measurements and log data to make the bulk density profile. In both holes, the upper part of the holes had deteriorated before we were able to conduct the logging runs; they had washed out to be wider than the caliper holding the HLDT density tool against the borehole wall. The tool sensor then periodically rode away from the wall out into the borehole and logged a combination of borehole water and sediment. Low bulk density readings result from the washouts. Accordingly, we constructed composite sections by using shipboard physical properties to 235.8 mbsf at Site 803 and to 320 mbsf at Site 806. Below these depths the logging bulk densities were used. The records were then interpolated to an even sample interval (0.5-m spacing at Site 806; 0.25-m spacing at Site 803) for the inverse signal correlation.

Sites 806 and 805

The results of the correlation are shown in Figures 11A and 12 and in Table 1. The map between Sites 806 and 805 is not nearly so linear as those from the top of the plateau. Kinks in the correlation map are well constrained, however, as is shown in Figure 13. The match with biostratigraphy is very good, in part because we redid the correlation repeatedly when early versions did not match as well. The section most difficult to match was that at about 300 mbsf equivalent depth in Site 806 (Fig. 11A). The basic offset between the two records caused amplitudes of equivalent peaks to match poorly and made the correlation ambiguous. Nevertheless, with a sufficient number of trials, we did manage to achieve a believable correlation between the two drill sites.

Sites 807 and 803

Correlating Sites 807 and 803 by means of the bulk density profiles was straightforward (Fig. 11B). The results, shown in Figure 14 and in Table 2, match the calcareous nannofossil stratigraphy of Takayama and Backman (this volume). The section between 200 and 300 mbsf in Hole 803D is offset from the biostratigraphic correlation between the two holes by about 10 m, but we could not find any good way to change the bulk density correlation.

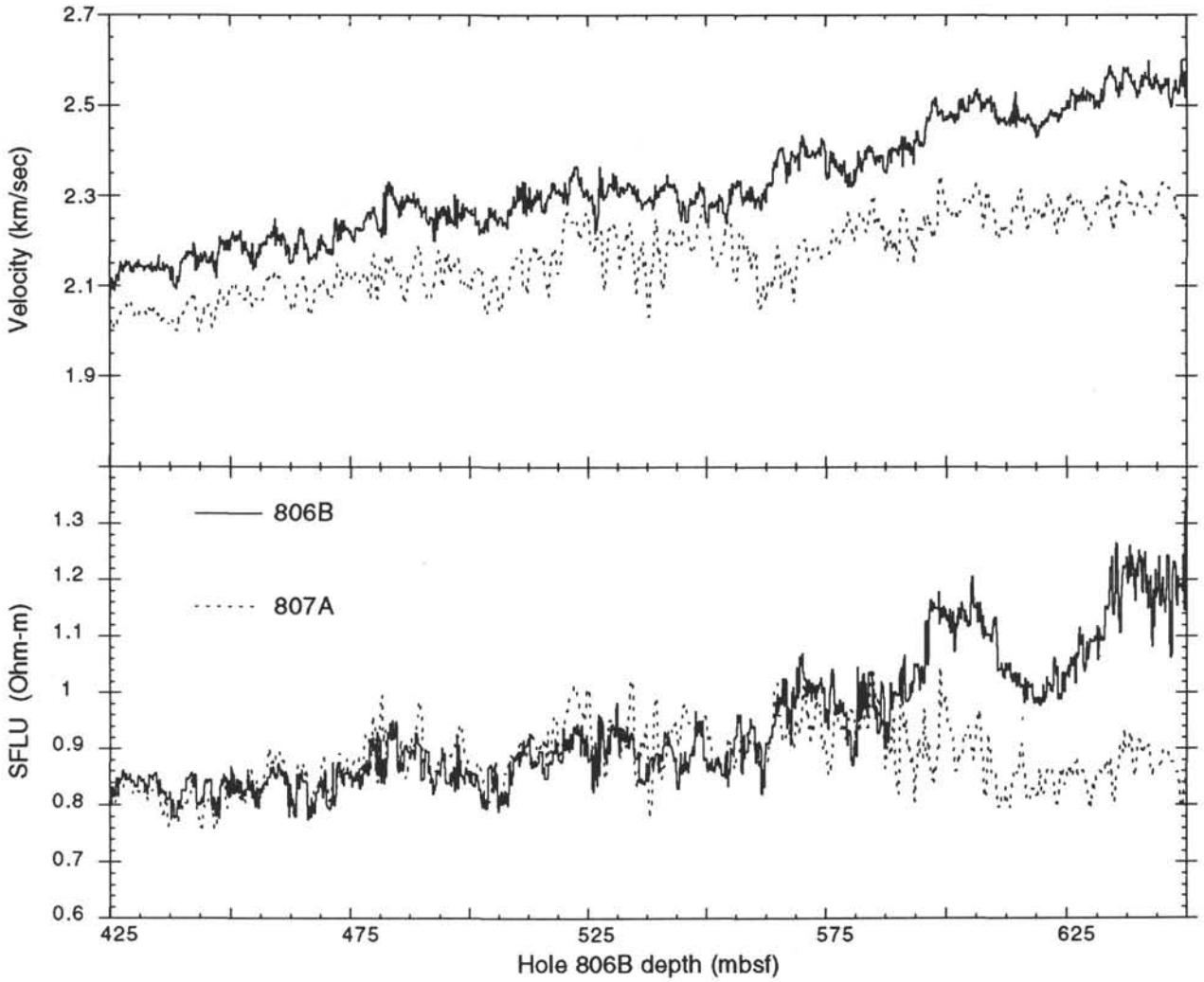

Figure 5. A comparison between Holes 806B and 807A of the velocity and SFLU resistivity logs. The interval above about 520 mbsf is well correlated; below this depth (about 14.9 Ma), however, the records are divergent. It is unknown at this time why they diverge, but the cause may relate to the equatorial crossing of Site 807 at about 14.4 Ma.

Latitudinal Effects upon Ontong Java Plateau Sedimentation

We plotted two separate panels for Figure 11 to emphasize that, although these sites were drilled to be part of a single depth transect, obvious common latitudinal variations in sedimentation are present. Sites 807 and 803 are the two northernmost sites (Fig. 1), and they have a common bulk density profile marked most prominently by a flattening of the profile deeper than about 500 m equivalent depth in Site 806. They also have higher bulk density excursions at 300 m and at about 420 m equivalent depth when compared with the southern sites. Sites to the south, including Site 586, have roughly linear bulk density profiles with depth and very low bulk density excursions. For this reason, when we compare fluctuations in sedimentation down the flank of the plateau in the next section, we compare Site 803 to Site 807 and the other drill sites to Site 806.

SEDIMENTATION RATE FLUCTUATIONS AND CCD CHANGES IN THE WESTERN EQUATORIAL PACIFIC OCEAN

Part of the rationale for drilling the Leg 130 sites was to examine calcium carbonate dissolution through time for this western equatorial Pacific transect. The drill sites extend down the flank of the Ontong Java Plateau from 2.6 km (the Holocene top of the lysocline) to just above the typical glacial top of the lysocline at about 3.6 km (Wu et al., 1991). Because the sediments are roughly 90% calcium carbonate, and because we can see little or no systematic variation of carbonate content down the flank of the plateau (Kroenke, Berger, Janecek, et al., 1991), relative sedimentation rates should to a first approximation reflect changes in calcite dissolution down the flanks. A relative sedimentation rate is the amount of sediment accumulated at one of the flank sites (805 and 803) divided by the amount of sediment accumulated during the same time period at a reference site on top of the plateau, where we assume that no dissolution has occurred. When the relative sediment accumulation equals 1, the flank site and the reference site have the same sedimentation rate, and no dissolution has occurred, whereas a relative accumulation of 0 indicates that the flank site experienced a hiatus.

Figure 15 summarizes the variations we found. Plotted on the figure are the relative rates of accumulation at Sites 803 and 805 and CCD variations from the central Pacific for both equatorial DSDP drill sites (within 3° of the equator) and nonequatorial sites. The CCD depth has been inverted on the figure, so that changes in the plotted CCD should have the same sense of change as changes in dissolution recorded by the relative sedimentation rates. Site 803 has changes in relative sediment accumulation that vaguely resemble changes in

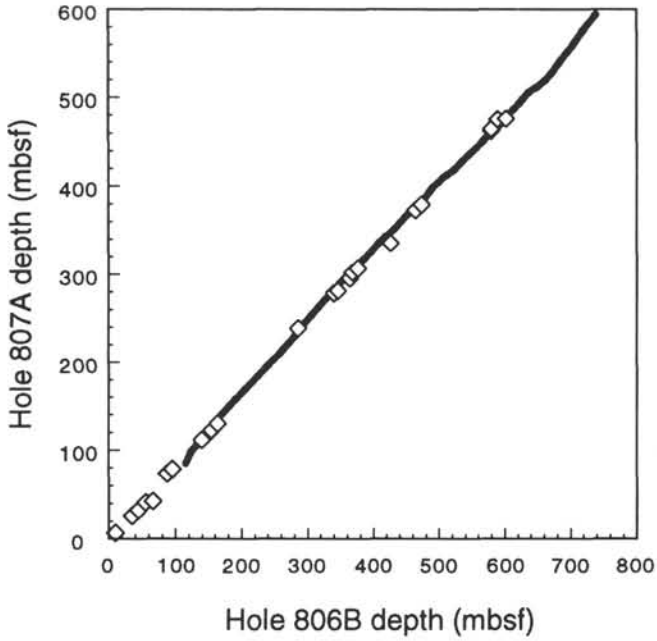

Figure 6. Correlation between Holes 806B and 807A, showing the inverse signal correlation map (solid line) compared to the biostratigraphic events found from the detailed post-cruise analysis of nannofossils (Takayama and Backman, this volume).

equatorial CCD, at least for the last 40 m.y. of Earth's history. At about 34 Ma, when the Pacific experienced its deepest CCD, Site 803 accumulated almost as much sediment as Site 807 on top of the Ontong Java Plateau. The relative accumulation rate dropped through time so that by the early Miocene, at about 20 Ma, Site 803 was accumulating only about one third as much sediment as Site 807. This was also a period when the CCD was relatively deep. From the middle to late Miocene, the relative accumulation of sediment at Site 803 slowly increased. In this interval, however, the equatorial CCD has stayed relatively flat. If these changes of relative sediment accumulation represent changes in dissolution, the western equatorial Pacific has a different carbonate dissolution history than the central Pacific.

The relative accumulation history of Site 805 makes us question whether the sedimentation rates on the flank of the Ontong Java Plateau are controlled by carbonate dissolution. Because it is compared with Site 806, we have only a Neogene record of relative sediment accumulation. Nevertheless, Site 805 has its own unique pattern of deposition. Roughly every 5 m.y., Site 805 went through a sedimentation cycle, alternating between low sedimentation rates, similar to Site 803, and high sedimentation rates comparable to Site 806, on top of the plateau. These cycles are insensitive to the correlation between Sites 806 and 805. Repeated attempts to redo the correlation could not eliminate the cycles, and only managed to move their location in time slightly. At Site 805 two peaks of relatively high sediment accumulation occurred during the early Miocene interval during which Site 803 was accumulating sediments most slowly and when Site 804 experienced a hiatus. Thus, sediment accumulation patterns opposite in sign occurred within a 200-m depth window. If this pattern is caused by dissolution, the lysocline must have become an extremely narrow horizon during these Miocene intervals.

The variations we have observed in relative sediment accumulation at Site 805 were not driven by cessation of sedimentation on top of the Ontong Java Plateau. Figure 16 plots sedimentation rates for Sites 803, 805, and 806 and the CCD profiles. The interval at about 20 Ma at Site 806 is marked by the lowest sedimentation rates in the entire cored section, but the sedimentation rate never dropped below 10 m/m.y. The sedimentation rates at Site 805 oscillated fairly wildly during this time period. Thus, the oscillations at Site 805, not the sedimentation changes on top of the plateau, cause the pattern of relative sediment accumulation at Site 805.

Comparing the complete profiles of sedimentation rate makes it clear that the absolute sedimentation rate over the entire Ontong Java Plateau was not driven by CCD changes but by other external factors in the carbon cycle. During the Miocene, when the central Pacific CCD experienced trends toward shallower CCDs (more dissolution), the sediments on the plateau first experienced a minimum in sedimentation centered about 20 Ma, and then experienced oscillatory, but generally increasing sedimentation rates throughout the rest of the period. Rates of inorganic carbon burial on the plateau increased dramatically, therefore, because the calcite contents of the sediments hardly varied from 90% (Kroenke, Berger, Janecek, et al., 1991).

CONCLUSIONS

Well logs have provided a means to correlate drill sites rapidly on the Ontong Java Plateau at a scale of meters or less. The logs are sufficiently reproducible to allow even subtle features to be correlated. On top of the plateau variations in sediment resistivity, which represent minor porosity variations, could be correlated across almost 500 km between sites. The quality of the correlations emphasize the uniform nature of sedimentation on top of the plateau and point out that winnowing events, if they occur, must be plateau-wide and not local sedimentation events.

We naively assumed, when we started this study, that correlating among drill sites down the flank of the Ontong Java Plateau would provide us with information that could easily be interpreted as dissolution variations caused by fluctuations in the western Pacific lysocline and CCD. We found, however, that some of the variations we observed were opposite in sign for adjacent sites. In particular, Site 803, at 3.4 km, and Site 805, at 3.2 km, accumulate sediment in different patterns through time. If the difference in sedimentation between these two sites is controlled largely by dissolution, then periods between 15 and 20 Ma are present in which the lysocline must have thinned substantially, when there would have been almost a steplike transition between sediments that accumulated carbonate and those that did not. These "narrow lysocline" periods occur when Neogene sedimentation rates were the lowest; thus, they may represent a rising of the CCD caused by low inorganic carbon supply to the oceans. Alternatively, the change in relative sedimentation rates may be unrelated to deposition and may merely represent local variations in sediment deposition on the topographically complex flank of the Ontong Java Plateau. High-resolution interpretations of seismic reflection records along the flank of the plateau, or further drilling, will allow us to choose between these two alternatives.

REFERENCES

Berger, W.H., 1973. Cenozoic sedimentation in the eastern tropical Pacific. *Geol. Soc. Am. Bull.*, 84:1941–1954.

Imbrie, J., Hays, J.D., Martinson, D.G., McIntyre, A., Mix, A.C., Morley, J.J., Pisias, N.G., Prell, W.L., and Shackleton, N.J., 1984. The orbital theory of Pleistocene climate: support from a revised chronology of the marine $\delta^{18}O$ record. *In* Berger, A.L., Imbrie, J., Hays, J., Kukla, G., and Saltzman, B. (Eds.), *Milankovitch and Climate* (Pt. 1): Dordrecht (D. Reidel), 269–305.

Kroenke, L.W., Berger, W.H., Janecek, T.R., et al., 1991. *Proc. ODP, Init. Repts.*, 130: College Station TX (Ocean Drilling Program).

Martinson, D.G., Menke, W., and Stoffa, P., 1982. An inverse approach to signal correlation. *J. Geophys. Res.*, 87:4807–4818.

Martinson, D.G., Pisias, N.G., Hays, J.D., Imbrie, J., Moore, T.C., Jr., and Shackleton, N.J., 1987. Age dating and the orbital theory of the ice ages: development of a high resolution 0 to 300,000-year chronostratigraphy. *Quat. Res.*, 27:1–29.

Mayer, L.A., Shipley, T.H., Winterer, E.L., Mosher, D., and Hagen, R.A, 1991. SeaBeam and seismic reflection surveys on the Ontong Java Plateau. *In* Kroenke, L.W., Berger, W.H., Janecek, T.R., et al., 1991. *Proc. ODP, Init. Repts.*, 130: College Station TX (Ocean Drilling Program), 45–75.

Moberly, R., Schlanger, S.O., et al., 1986. *Init. Repts. DSDP,* 89: Washington (U.S. Govt. Printing Office).
Resig, J., Buyannanonth, V., and Roy, K., 1976. Foraminiferal stratigraphy and depositional history of the Ontong Java Plateau. *Deep-Sea Res.*, 23:441–456.
Shackleton, N.J., et al., 1984. Oxygen isotope calibration of the onset of ice-rafting and history of glaciation in the North Atlantic region. *Nature,* 307:620–623.
van Andel, T.H., Heath, G.R., and Moore, T.C., Jr., 1975. Cenozoic history and paleoceanography of the central equatorial Pacific Ocean. *Geol Soc. Am. Mem.,* 143.
van Andel, T.H., and Moore, T.C., Jr., 1974. Cenozoic calcium carbonate distribution and calcite compensation depth in the central equatorial Pacific Ocean. *Geology,* 2:87–92.
Wu, G., Yasuda, M.K., and Berger, W.H., 1991. Late Pleistocene carbonate stratigraphy on Ontong-Java Plateau in the western equatorial Pacific. *Mar. Geol.,* 99:135–150.

Date of initial receipt: 21 October 1991
Date of acceptance: 19 June 1992
Ms 130B-043

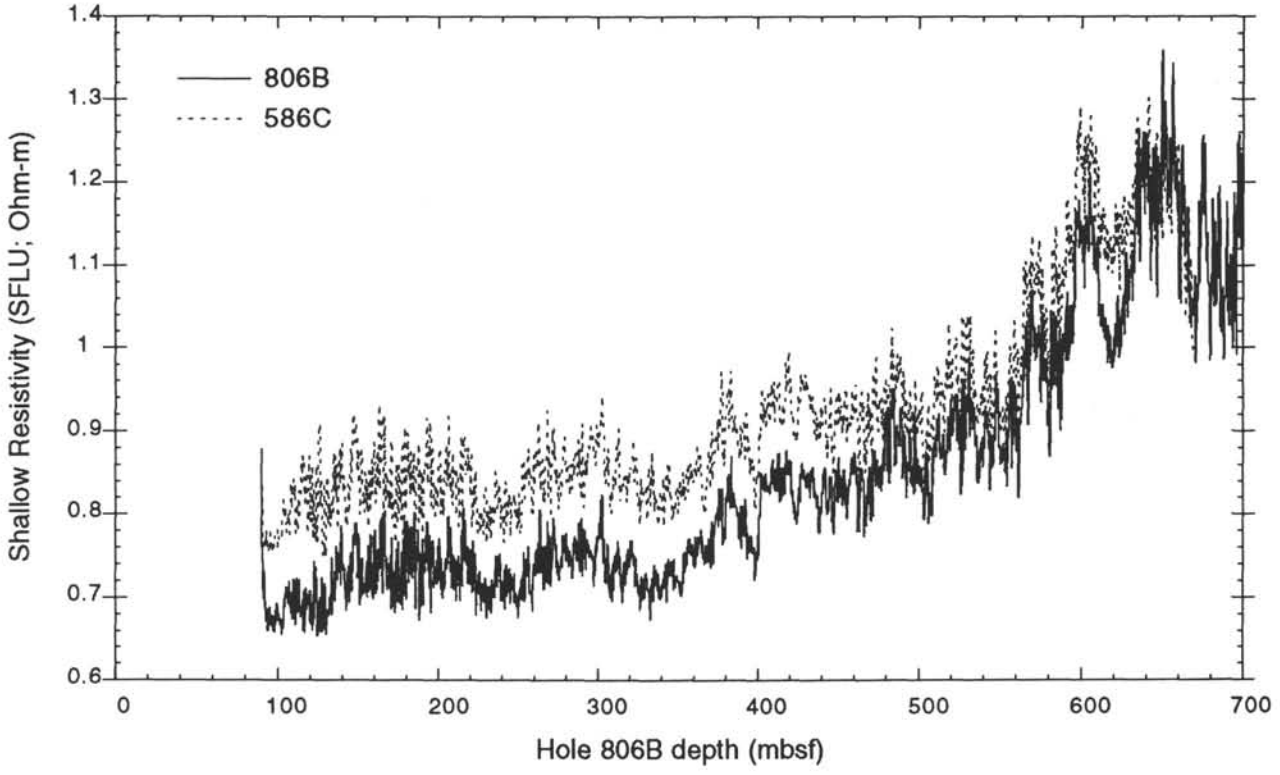

Figure 7. SFLU shallow resistivity well logs for Holes 806B and 586C, about 75 nmi apart, plotted on the correlation depth scale of Hole 806B. Note the high coherence for the entire length of the records. The offset between the two logs is a result of uncorrected borehole size effects.

Table 1. Equivalent depths at drill sites on the Ontong Java Plateau.

Hole 806B		Hole 586C	Hole 807A	Hole 805C	Hole 803D	Hole 806B		Hole 586C	Hole 807A	Hole 805C	Hole 803D
Depth (mbsf)	Age (Ma)	Depth (mbsf)	Depth (mbsf)	Depth (mbsf)	Depth (mbsf)	Depth (mbsf)	Age (Ma)	Depth (mbsf)	Depth (mbsf)	Depth (mbsf)	Depth (mbsf)
90.0	3.426	95.55				164.0	5.040	159.82	134.86	124.41	
91.0	3.448	96.28				165.0	5.062	160.66	136.08	125.19	
92.0	3.469	96.85				166.0	5.084	161.49	137.31	125.97	
93.0	3.491	97.42				167.0	5.105	162.39	138.32	126.74	
94.0	3.513	97.99				168.0	5.127	163.30	139.09	127.41	73.86
95.0	3.535	98.55				169.0	5.149	164.21	139.88	128.09	74.40
96.0	3.557	99.12				170.0	5.171	165.10	140.66	128.77	74.94
97.0	3.578	99.69				171.0	5.193	166.01	141.44	129.46	75.47
98.0	3.600	100.26				172.0	5.214	166.91	142.21	130.15	76.01
99.0	3.622	100.84				173.0	5.236	167.80	143.03	130.84	76.57
100.0	3.644	101.41				174.0	5.258	168.71	143.91	131.54	77.18
101.0	3.666	101.98				175.0	5.280	169.60	144.77	132.24	77.78
102.0	3.688	102.55				176.0	5.302	170.50	145.64	132.95	78.38
103.0	3.709	103.12				177.0	5.324	171.39	146.51	133.69	78.98
104.0	3.731	103.69				178.0	5.345	172.29	147.37	134.53	79.57
105.0	3.753	104.56				179.0	5.367	173.18	148.24	135.37	80.17
106.0	3.775	105.53				180.0	5.389	174.06	149.10	136.23	80.77
107.0	3.797	106.51				181.0	5.411	174.96	149.95	137.09	81.36
108.0	3.818	107.48				182.0	5.433	175.85	150.82	137.95	81.95
109.0	3.840	108.46				183.0	5.454	176.73	151.68	138.82	82.55
110.0	3.862	109.43				184.0	5.476	177.62	152.55	139.70	83.15
111.0	3.884	110.41				185.0	5.498	178.50	153.42	140.57	83.75
112.0	3.906	111.40				186.0	5.520	179.39	154.22	141.45	84.32
113.0	3.927	112.37				187.0	5.542	180.27	154.96	142.33	84.81
114.0	3.949	113.36				188.0	5.563	181.14	155.69	143.21	85.31
115.0	3.971	114.34	84.92			189.0	5.585	182.04	156.43	144.08	85.83
116.0	3.993	115.33	86.19			190.0	5.607	182.91	157.17	144.96	86.34
117.0	4.015	116.31	87.46			191.0	5.629	183.79	157.91	145.76	86.85
118.0	4.037	117.30	88.72			192.0	5.651	184.67	158.65	146.54	87.38
119.0	4.058	118.29	90.22			193.0	5.673	185.54	159.44	147.31	87.92
120.0	4.080	119.28	92.12			194.0	5.694	186.43	160.25	148.08	88.47
121.0	4.102	120.28	94.01			195.0	5.716	187.31	161.05	148.84	89.03
122.0	4.124	121.27	95.89			196.0	5.738	188.18	161.85	149.59	89.59
123.0	4.146	122.26	97.76			197.0	5.760	189.06	162.66	150.33	90.16
124.0	4.167	123.26	98.81			198.0	5.782	189.93	163.47	151.07	90.72
125.0	4.189	124.26	99.69			199.0	5.803	190.81	164.29	151.82	91.27
126.0	4.211	125.25	100.57			200.0	5.825	191.69	165.10	152.57	91.85
127.0	4.233	126.26	101.44			201.0	5.847	192.56	165.92	153.30	92.42
128.0	4.255	127.26	102.29			202.0	5.869	193.44	166.74	154.03	92.98
129.0	4.276	128.27	103.14			203.0	5.891	194.32	167.54	154.74	93.56
130.0	4.298	129.28	103.96			204.0	5.912	195.20	168.35	155.45	94.12
131.0	4.320	130.28	104.78			205.0	5.934	196.07	169.15	156.14	94.67
132.0	4.342	131.30	105.59			206.0	5.956	196.94	169.94	156.83	95.23
133.0	4.364	132.30	106.39			207.0	5.978	197.83	170.73	157.51	95.78
134.0	4.386	133.32	107.19			208.0	6.000	198.70	171.51	158.18	96.32
135.0	4.407	134.34	107.97			209.0	6.022	199.58	172.30	158.85	96.87
136.0	4.429	135.35	108.75			210.0	6.043	200.46	173.08	159.50	97.42
137.0	4.451	136.38	109.54			211.0	6.065	201.32	173.86	160.15	97.97
138.0	4.473	137.39	110.31			212.0	6.087	202.21	174.63	160.80	98.52
139.0	4.495	138.41	111.07			213.0	6.109	203.08	175.46	161.44	99.08
140.0	4.516	139.44	111.87			214.0	6.131	203.96	176.27	162.08	99.65
141.0	4.538	140.30	112.59			215.0	6.152	204.84	177.06	162.72	100.21
142.0	4.560	141.14	113.31			216.0	6.174	205.71	177.86	163.35	100.77
143.0	4.582	141.99	114.03			217.0	6.196	206.55	178.66	163.98	101.34
144.0	4.604	142.84	114.76			218.0	6.218	207.40	179.46	164.61	101.92
145.0	4.625	143.68	115.49			219.0	6.240	208.24	180.25	165.24	102.48
146.0	4.647	144.53	116.23			220.0	6.261	209.09	181.04	165.87	103.05
147.0	4.669	145.38	117.35			221.0	6.283	209.94	181.83	166.50	103.62
148.0	4.691	146.23	118.49			222.0	6.305	210.78	182.62	167.13	104.19
149.0	4.713	147.08	119.66			223.0	6.327	211.62	183.40	167.77	104.75
150.0	4.735	147.93	120.89			224.0	6.349	212.48	184.19	168.41	105.30
151.0	4.756	148.78	122.12			225.0	6.371	213.32	184.97	169.05	105.87
152.0	4.778	149.63	123.29			226.0	6.392	214.16	185.75	169.70	106.43
153.0	4.800	150.47	124.08			227.0	6.414	215.02	186.52	170.35	106.98
154.0	4.822	151.33	124.88			228.0	6.436	215.86	187.29	171.01	107.53
155.0	4.844	152.18	125.69			229.0	6.458	216.71	188.07	171.68	108.08
156.0	4.865	153.03	126.51			230.0	6.480	217.56	188.84	172.35	108.64
157.0	4.887	153.87	127.34			231.0	6.501	218.40	189.60	173.03	109.19
158.0	4.909	154.73	128.18			232.0	6.523	219.24	190.37	173.71	109.74
159.0	4.931	155.58	129.03			233.0	6.545	220.10	191.13	174.41	110.29
160.0	4.953	156.43	130.02			234.0	6.567	220.94	191.89	175.11	110.84
161.0	4.975	157.27	131.21			235.0	6.589	221.79	192.65	175.82	111.37
162.0	4.996	158.12	132.43	122.86		236.0	6.610	222.64	193.42	176.54	111.92
163.0	5.018	158.96	133.64	123.64		237.0	6.632	223.48	194.16	177.27	112.46

Table 1 (continued).

Hole 806B		Hole 586C	Hole 807A	Hole 805C	Hole 803D	Hole 806B		Hole 586C	Hole 807A	Hole 805C	Hole 803D
Depth (mbsf)	Age (Ma)	Depth (mbsf)	Depth (mbsf)	Depth (mbsf)	Depth (mbsf)	Depth (mbsf)	Age (Ma)	Depth (mbsf)	Depth (mbsf)	Depth (mbsf)	Depth (mbsf)
238.0	6.654	224.33	194.92	178.01	113.00	312.0	8.268	288.01	259.00	234.18	161.71
239.0	6.676	225.18	195.72	178.76	113.56	313.0	8.290	288.90	259.89	235.07	162.26
240.0	6.698	226.02	196.53	179.51	114.14	314.0	8.312	289.80	260.81	235.96	162.84
241.0	6.720	226.86	197.32	180.28	114.71	315.0	8.334	290.69	261.70	236.84	163.41
242.0	6.741	227.72	198.11	181.05	115.27	316.0	8.356	291.58	262.60	237.72	163.98
243.0	6.763	228.56	198.89	181.83	115.83	317.0	8.377	292.48	263.48	238.59	164.55
244.0	6.785	229.41	199.70	182.62	116.39	318.0	8.399	293.36	264.35	239.45	165.11
245.0	6.807	230.25	200.48	183.42	116.95	319.0	8.421	294.26	265.23	240.38	165.68
246.0	6.829	231.09	201.26	184.21	117.51	320.0	8.443	295.14	266.09	241.44	166.24
247.0	6.850	231.94	202.04	184.99	118.07	321.0	8.465	296.03	266.97	242.49	166.81
248.0	6.872	232.79	202.83	185.78	118.62	322.0	8.486	296.92	267.83	243.53	167.36
249.0	6.894	233.63	203.61	186.57	119.17	323.0	8.508	297.79	268.72	244.56	167.95
250.0	6.916	234.48	204.38	187.37	119.72	324.0	8.530	298.68	269.53	245.59	168.48
251.0	6.938	235.33	205.16	188.17	120.28	325.0	8.552	299.57	270.29	246.58	168.96
252.0	6.959	236.17	205.95	188.97	120.82	326.0	8.574	300.45	271.05	247.46	169.48
253.0	6.981	237.01	206.72	189.78	121.36	327.0	8.595	301.34	271.83	248.31	169.99
254.0	7.003	237.86	207.39	190.59	121.84	328.0	8.617	302.21	272.62	249.15	170.51
255.0	7.025	238.71	208.03	191.40	122.28	329.0	8.639	303.09	273.42	249.90	171.04
256.0	7.047	239.55	208.68	192.21	122.75	330.0	8.661	303.98	274.23	250.61	171.59
257.0	7.069	240.40	209.51	193.03	123.32	331.0	8.683	304.85	275.06	251.60	172.14
258.0	7.090	241.25	210.38	193.84	123.94	332.0	8.705	305.73	275.91	252.59	172.70
259.0	7.112	242.09	211.24	194.65	124.53	333.0	8.726	306.62	276.75	253.58	173.27
260.0	7.134	242.95	212.09	195.47	125.14	334.0	8.760	307.49	277.60	254.57	173.84
261.0	7.156	243.79	212.95	196.28	125.72	335.0	8.802	308.38	278.47	255.57	174.42
262.0	7.178	244.64	213.79	197.09	126.31	336.0	8.844	309.25	279.34	256.57	175.01
263.0	7.199	245.50	214.63	197.90	126.90	337.0	8.885	310.13	280.22	257.58	175.61
264.0	7.221	246.34	215.48	198.71	127.49	338.0	8.927	311.01	281.10	258.59	176.21
265.0	7.243	247.20	216.32	199.52	128.07	339.0	8.969	311.88	281.98	260.19	176.81
266.0	7.265	248.05	217.17	200.33	128.66	340.0	9.011	312.77	282.86	262.07	177.41
267.0	7.287	248.90	218.01	201.14	129.24	341.0	9.052	313.64	283.75	263.96	178.01
268.0	7.309	249.74	218.87	201.94	129.83	342.0	9.094	314.53	284.72	265.43	178.68
269.0	7.330	250.60	219.71	202.75	130.56	343.0	9.136	315.42	285.69	266.40	179.34
270.0	7.352	251.46	220.58	203.55	131.33	344.0	9.178	316.29	286.65	267.28	179.99
271.0	7.374	252.32	221.43	204.40	132.10	345.0	9.220	317.17	287.48	267.80	180.58
272.0	7.396	253.17	222.30	205.26	132.88	346.0	9.261	318.06	288.29	268.33	181.12
273.0	7.418	254.02	223.20	206.12	133.67	347.0	9.303	318.93	289.10	268.87	181.68
274.0	7.439	254.88	224.10	206.98	134.49	348.0	9.345	319.83	289.89	269.40	182.22
275.0	7.461	255.74	225.02	207.84	135.32	349.0	9.387	320.71	290.68	269.93	182.76
276.0	7.483	256.59	225.95	208.69	136.14	350.0	9.429	321.59	291.45	270.47	183.30
277.0	7.505	257.45	226.88	209.55	136.98	351.0	9.470	322.48	292.23	271.00	183.84
278.0	7.527	258.32	227.83	210.31	137.81	352.0	9.512	323.36	293.00	271.54	184.38
279.0	7.548	259.17	228.79	210.75	138.67	353.0	9.554	324.25	293.76	272.07	184.89
280.0	7.570	260.04	229.72	211.20	139.51	354.0	9.596	325.14	294.51	272.60	185.42
281.0	7.592	260.90	230.66	211.64	140.33	355.0	9.637	326.02	295.26	273.12	185.94
282.0	7.614	261.76	231.61	212.08	141.20	356.0	9.679	326.92	296.01	273.65	186.46
283.0	7.636	262.62	232.59	212.52	142.05	357.0	9.721	327.81	296.76	274.17	186.97
284.0	7.658	263.48	233.57	212.97	142.92	358.0	9.763	328.70	297.51	274.65	187.49
285.0	7.679	264.35	234.57	213.41	143.82	359.0	9.805	329.59	298.27	275.08	188.01
286.0	7.701	265.21	235.57	213.85	144.70	360.0	9.846	330.49	299.02	275.50	188.54
287.0	7.723	266.07	236.52	214.29	145.54	361.0	9.888	331.39	299.78	275.93	189.08
288.0	7.745	266.94	237.43	214.73	146.36	362.0	9.930	332.27	300.55	276.35	189.60
289.0	7.767	267.80	238.37	215.30	147.21	363.0	9.972	333.17	301.33	276.77	190.14
290.0	7.788	268.66	239.31	215.87	148.03	364.0	10.013	334.07	302.11	277.19	190.68
291.0	7.810	269.52	240.25	216.44	148.87	365.0	10.055	334.97	302.90	277.60	191.22
292.0	7.832	270.39	241.21	217.01	149.73	366.0	10.097	335.87	303.72	278.02	191.79
293.0	7.854	271.25	242.17	217.57	150.59	367.0	10.139	336.76	304.53	278.44	192.35
294.0	7.876	272.11	243.12	218.14	151.44	368.0	10.181	337.67	305.29	278.85	192.87
295.0	7.897	272.97	244.08	218.70	152.29	369.0	10.222	338.56	305.98	279.26	193.35
296.0	7.919	273.83	245.03	219.26	153.09	370.0	10.264	339.47	306.66	279.68	193.84
297.0	7.941	274.70	245.98	219.82	153.65	371.0	10.306	340.37	307.36	280.09	194.31
298.0	7.963	275.55	246.91	220.38	154.21	372.0	10.348	341.27	308.07	280.50	194.78
299.0	7.985	276.41	247.81	221.01	154.76	373.0	10.390	342.18	308.78	280.92	195.28
300.0	8.007	277.27	248.65	221.65	155.28	374.0	10.431	343.08	309.49	281.33	195.74
301.0	8.028	278.12	249.47	222.80	155.76	375.0	10.473	343.99	310.21	281.75	196.14
302.0	8.050	278.99	250.32	223.94	156.30	376.0	10.515	344.89	310.92	282.17	196.48
303.0	8.072	279.89	251.29	225.08	156.90	377.0	10.557	345.81	311.63	282.59	196.86
304.0	8.094	280.79	252.22	226.21	157.46	378.0	10.598	346.71	312.35	283.01	197.24
305.0	8.116	281.70	253.14	227.34	158.03	379.0	10.640	347.62	313.06	283.44	197.60
306.0	8.137	282.60	254.02	228.46	158.58	380.0	10.682	348.53	313.78	283.87	197.98
307.0	8.159	283.51	254.90	229.57	159.13	381.0	10.724	349.44	314.49	284.30	198.34
308.0	8.181	284.41	255.75	230.54	159.66	382.0	10.766	350.35	315.20	284.73	198.71
309.0	8.203	285.31	256.58	231.46	160.19	383.0	10.807	351.26	315.90	285.17	199.09
310.0	8.225	286.22	257.41	232.37	160.70	384.0	10.849	352.18	316.61	285.62	199.46
311.0	8.246	287.11	258.22	233.28	161.20	385.0	10.891	353.08	317.31	286.06	199.82

Table 1 (continued).

Hole 806B		Hole 586C	Hole 807A	Hole 805C	Hole 803D	Hole 806B		Hole 586C	Hole 807A	Hole 805C	Hole 803D
Depth (mbsf)	Age (Ma)	Depth (mbsf)	Depth (mbsf)	Depth (mbsf)	Depth (mbsf)	Depth (mbsf)	Age (Ma)	Depth (mbsf)	Depth (mbsf)	Depth (mbsf)	Depth (mbsf)
386.0	10.933	354.00	318.01	286.51	200.19	513.0	14.524	469.70	413.24	360.15	242.01
387.0	10.975	354.91	318.71	286.97	200.55	514.0	14.582	470.61	413.76	361.20	242.18
388.0	11.016	355.82	319.40	287.43	200.91	515.0	14.640	471.54	414.27	362.39	242.37
389.0	11.058	356.73	320.10	287.89	201.27	516.0	14.697	472.45	414.77	363.58	242.56
390.0	11.100	357.64	320.80	288.36	201.64	517.0	14.755	473.37	415.28	364.77	242.74
391.0	11.142	358.56	321.50	288.83	202.00	518.0	14.813	474.27	415.79	365.94	242.91
392.0	11.183	359.47	322.20	289.31	202.36	519.0	14.870	475.19	416.31	367.10	243.10
393.0	11.225	360.39	322.89	289.79	202.73	520.0	14.928	476.11	416.81	368.24	243.28
394.0	11.267	361.29	323.60	290.27	203.09	521.0	14.986	477.03	417.32	369.34	243.46
395.0	11.309	362.21	324.30	290.76	203.45	522.0	15.043	477.95	417.87	370.04	243.67
396.0	11.351	363.12	325.01	291.25	203.81	523.0	15.101	478.86	418.66	370.52	243.95
397.0	11.392	364.03	325.71	291.74	204.19	524.0	15.159	479.79	419.46	370.99	244.25
398.0	11.434	364.94	326.42	292.23	204.55	525.0	15.217	480.70	420.27	371.44	244.54
399.0	11.476	365.85	327.24	292.73	204.95	526.0	15.274	481.63	421.07	371.88	244.83
400.0	11.518	366.77	328.14	293.23	205.43	527.0	15.332	482.55	421.88	372.30	245.13
401.0	11.559	367.67	329.02	293.72	205.88	528.0	15.390	483.47	422.68	372.70	245.41
402.0	11.601	368.59	329.89	294.22	206.33	529.0	15.447	484.39	423.48	373.09	245.71
403.0	11.643	369.50	330.77	294.72	206.77	530.0	15.505	485.31	424.29	373.45	246.00
404.0	11.685	370.40	331.63	295.22	207.21	531.0	15.563	486.24	425.08	373.85	246.30
405.0	11.727	371.33	332.51	295.71	207.66	532.0	15.620	487.17	425.88	374.23	246.60
406.0	11.768	372.23	333.37	296.21	208.10	533.0	15.678	488.10	426.68	374.60	246.89
407.0	11.810	373.14	334.24	296.71	208.54	534.0	15.736	489.02	427.48	374.95	247.18
408.0	11.852	374.05	335.10	297.20	208.98	535.0	15.793	489.96	428.27	375.28	247.48
461.0	13.350	422.14	374.09	325.48	227.82	536.0	15.851	490.88	429.06	375.59	247.78
462.0	13.366	423.04	374.73	326.04	228.05	537.0	15.909	491.82	429.80	375.89	248.05
463.0	13.383	423.97	375.35	326.59	228.29	538.0	15.966	492.74	430.52	376.18	248.33
464.0	13.399	424.88	375.97	327.14	228.53	539.0	16.004	493.67	431.25	376.45	248.60
465.0	13.415	425.80	376.62	327.68	228.77	540.0	16.043	494.60	431.97	376.72	248.88
466.0	13.431	426.71	377.31	329.16	229.03	541.0	16.081	495.54	432.69	376.97	249.14
467.0	13.447	427.63	378.01	330.85	229.29	542.0	16.119	496.47	433.41	377.21	249.41
468.0	13.464	428.54	378.72	332.49	229.56	543.0	16.158	497.39	434.12	377.45	249.69
469.0	13.480	429.46	379.44	334.07	229.83	544.0	16.196	498.33	434.83	377.67	249.96
470.0	13.496	430.38	380.16	335.61	230.10	545.0	16.234	499.26	435.54	377.89	250.23
471.0	13.512	431.29	380.91	337.11	230.38	546.0	16.272	500.20	436.25	378.11	250.51
472.0	13.528	432.22	381.69	338.56	230.67	547.0	16.311	501.13	436.96	378.31	250.78
473.0	13.545	433.12	382.48	339.84	230.97	548.0	16.349	502.06	437.66	378.52	251.05
474.0	13.561	434.05	383.28	340.00	231.26	549.0	16.387	502.98	438.37	378.71	251.32
475.0	13.577	434.96	384.10	340.26	231.57	550.0	16.426	503.92	439.07	378.91	251.59
476.0	13.593	435.88	384.91	340.50	231.86	551.0	16.464	504.85	439.77	379.10	251.86
477.0	13.609	436.80	385.76	340.74	232.17	552.0	16.502	505.78	440.46	379.29	252.13
478.0	13.626	437.71	386.60	340.98	232.49	553.0	16.540	506.71	441.15	379.48	252.40
479.0	13.642	438.64	387.45	341.22	232.80	554.0	16.579	507.63	441.85	379.66	252.67
480.0	13.658	439.55	388.44	341.46	233.14	555.0	16.617	508.57	442.54	379.85	252.93
481.0	13.674	440.47	389.48	341.69	233.53	556.0	16.655	509.49	443.22	380.03	253.22
482.0	13.690	441.39	390.50	341.98	233.90	557.0	16.694	510.41	443.91	380.21	253.55
483.0	13.707	442.31	391.53	342.32	234.27	558.0	16.732	511.33	444.59	380.39	253.87
484.0	13.723	443.22	392.52	342.67	234.63	559.0	16.770	512.26	445.30	380.63	254.20
485.0	13.739	444.14	393.52	343.02	234.99	560.0	16.808	513.17	446.01	380.88	254.53
486.0	13.755	445.05	394.49	343.37	235.34	561.0	16.847	514.10	446.72	381.13	254.87
487.0	13.771	445.98	395.44	343.73	235.67	562.0	16.885	515.02	447.42	381.39	255.21
488.0	13.788	446.89	396.36	344.11	236.00	563.0	16.923	515.93	448.12	381.65	255.54
489.0	13.804	447.80	397.27	344.49	236.33	564.0	16.961	516.85	448.83	381.92	255.87
490.0	13.820	448.72	398.14	344.89	236.64	565.0	17.000	517.77	449.55	382.23	256.18
491.0	13.836	449.63	399.00	345.30	236.94	566.0	17.038	518.77	450.34	382.55	256.42
492.0	13.852	450.54	399.76	345.73	237.21	567.0	17.076	519.78	451.13	382.88	256.62
493.0	13.869	451.46	400.45	346.06	237.46	568.0	17.115	520.78	451.92	383.22	256.85
494.0	13.885	452.37	401.11	346.27	237.69	569.0	17.153	521.78	452.70	383.57	257.07
495.0	13.901	453.29	401.77	346.63	237.92	570.0	17.191	522.77	453.48	383.93	257.30
496.0	13.917	454.20	402.41	347.23	238.15	571.0	17.229	523.77	454.27	384.31	257.51
497.0	13.933	455.11	403.04	347.85	238.37	572.0	17.268	524.76	454.91	384.70	257.69
498.0	13.950	456.02	403.67	348.48	238.60	573.0	17.306	525.75	455.43	385.10	257.85
499.0	13.966	456.94	404.27	349.14	238.84	574.0	17.344	526.74	455.95	385.51	258.00
500.0	13.982	457.85	405.08	349.80	239.10	575.0	17.383	527.73	456.48	385.93	258.14
501.0	13.998	458.77	405.87	350.49	239.39	576.0	17.421	528.72	457.00	386.36	258.29
502.0	14.014	459.68	406.65	351.20	239.66	577.0	17.459	529.70	457.52	386.79	258.44
503.0	14.031	460.59	407.42	351.93	239.93	578.0	17.497	530.69	458.04	387.24	258.59
504.0	14.047	461.50	408.17	352.67	240.20	579.0	17.536	531.66	458.56	387.68	258.74
505.0	14.063	462.40	408.92	353.44	240.46	580.0	17.574	532.65	459.09	388.14	258.89
506.0	14.121	463.32	409.66	354.22	240.72	581.0	17.612	533.62	459.61	388.60	259.03
507.0	14.178	464.23	410.21	355.02	240.94	582.0	17.650	534.60	460.13	389.59	259.18
508.0	14.236	465.15	410.72	355.84	241.11	583.0	17.689	535.58	460.65	390.59	259.32
509.0	14.294	466.05	411.23	356.68	241.28	584.0	17.727	536.55	461.17	391.54	259.47
510.0	14.351	466.97	411.73	357.53	241.46	585.0	17.765	537.52	461.76	392.11	259.66
511.0	14.409	467.89	412.23	358.39	241.65	586.0	17.804	538.49	462.78	392.67	259.92
512.0	14.467	468.79	412.74	359.27	241.83	587.0	17.842	539.47	463.80	393.23	260.21

Table 1 (continued).

Hole 806B		Hole 586C	Hole 807A	Hole 805C	Hole 803D	Hole 806B		Hole 586C	Hole 807A	Hole 805C	Hole 803D
Depth (mbsf)	Age (Ma)	Depth (mbsf)	Depth (mbsf)	Depth (mbsf)	Depth (mbsf)	Depth (mbsf)	Age (Ma)	Depth (mbsf)	Depth (mbsf)	Depth (mbsf)	Depth (mbsf)
588.0	17.880	540.44	464.82	393.78	260.50	664.0	22.568	616.39	520.84	449.67	279.79
589.0	17.918	541.41	465.84	394.34	260.78	665.0	22.610	617.39	521.71	450.29	280.12
590.0	17.957	542.38	466.86	394.89	261.07	666.0	22.652	618.40	522.57	450.90	280.47
591.0	17.995	543.35	467.88	395.43	261.36	667.0	22.694	619.42	523.43	451.50	280.81
592.0	18.033	544.32	468.91	395.97	261.64	668.0	22.736	620.42	524.29	452.10	281.15
593.0	18.072	545.30	469.92	396.51	261.93	669.0	22.778	621.40	525.14	452.68	281.50
594.0	18.138	546.26	470.94	397.05	262.20	670.0	22.820	622.37	526.00	453.26	281.85
595.0	18.204	547.24	471.97	397.60	262.49	671.0	22.862		526.85	453.84	282.19
596.0	18.270	548.20	472.98	398.21	262.76	672.0	22.904		527.79	454.41	282.58
597.0	18.336	549.17	474.01	398.77	263.05	673.0	22.946		528.92	454.97	283.04
598.0	18.402	550.15	475.02	399.34	263.33	674.0	22.988		530.05	455.54	283.50
599.0	18.468	551.11	476.05	399.90	263.61	675.0	23.030		531.17	456.13	283.96
600.0	18.534	552.09	476.85	400.46	263.83	676.0	23.072		532.29	456.73	284.46
601.0	18.600	553.06	477.53	401.03	264.01	677.0	23.114		533.30	457.33	285.19
602.0	18.666	554.04	478.21	401.59	264.20	678.0	23.156		534.31	457.92	285.87
603.0	18.732	555.01	478.89	402.17	264.40	679.0	23.199		535.32	458.52	286.56
604.0	18.798	556.00	479.58	402.74	264.63	680.0	23.241		536.34	459.12	287.26
605.0	18.864	556.96	480.25	403.33	264.88	681.0	23.283		537.36	459.72	287.96
606.0	18.930	557.95	480.95	403.92	265.13	682.0	23.325		538.37	460.35	288.66
607.0	18.996	558.92	481.66	404.52	265.39	683.0	23.367		539.39	461.00	289.36
608.0	19.062	559.91	482.42	405.13	265.66	684.0	23.409		540.40	461.66	290.07
609.0	19.128	560.89	483.18	405.76	265.94	685.0	23.451		541.42	462.32	290.77
610.0	19.194	561.88	483.93	406.41	266.21	686.0	23.493		542.44	462.98	291.48
611.0	19.260	562.86	484.70	407.07	266.48	687.0	23.535		543.41	463.65	292.15
612.0	19.326	563.85	485.47	407.74	266.76	688.0	23.577		544.37	464.33	292.82
613.0	19.392	564.84	486.23	408.44	267.03	689.0	23.619		545.32	465.01	293.48
614.0	19.458	565.83	486.99	409.16	267.31	690.0	23.661		546.27	465.70	294.14
615.0	19.524	566.82	487.76	409.91	267.58	691.0	23.703		547.23	466.43	294.82
616.0	19.590	567.81	488.55	410.68	267.86	692.0	23.745		548.20	467.28	295.48
617.0	19.656	568.81	489.33	411.48	268.14	693.0	23.787		549.16	468.14	296.15
618.0	19.722	569.80	490.11	412.31	268.42	694.0	23.830		550.13	469.00	296.82
619.0	19.788	570.80	490.89	413.17	268.70	695.0	23.872		551.09	469.87	297.50
620.0	19.854	571.81	491.68	414.07	268.98	696.0	23.914		552.07	470.76	298.18
621.0	19.920	572.81	492.48	415.00	269.26	697.0	23.956		553.04	471.63	298.85
622.0	19.986	573.81	493.27	415.97	269.55	698.0	23.998		553.89	472.50	299.44
623.0	20.052	574.81	494.07	416.97	269.84	699.0	24.040		554.74	473.39	300.00
624.0	20.118	575.82	494.89	417.99	270.13	700.0	24.082		555.58	474.29	300.63
625.0	20.184	576.82	495.70	419.01	270.41	701.0	24.124		556.68	475.19	301.35
626.0	20.250	577.84	496.51	419.98	270.70	702.0	24.166		557.79	476.10	302.10
627.0	20.316	578.85	497.33	420.97	271.00	703.0	24.208		558.89	477.02	302.86
628.0	20.382	579.85	498.17	421.99	271.30	704.0	24.250		560.00	477.93	303.61
629.0	20.448	580.87	499.00	423.04	271.60	705.0	24.292		561.12	478.86	304.37
630.0	20.514	581.88	499.83	424.10	271.90	706.0	24.334		562.23	479.78	305.11
631.0	20.580	582.90	500.68	425.19	272.20	707.0	24.376		563.33		305.86
632.0	20.647	583.92	501.52	426.29	272.51	708.0	24.418		564.45		306.60
633.0	20.713	584.92	502.37	427.40	272.82	709.0	24.460		565.56		307.34
634.0	20.779	585.95	503.23	428.52	273.14	709.0	24.460		565.56		307.34
635.0	20.845	586.97	504.09	429.64	273.45	710.0	24.503		566.67		308.06
636.0	20.911	587.98	504.96	430.77	273.77	711.0	24.545		567.76		308.80
637.0	20.977	589.00	505.57	431.89	274.00	712.0	24.587		568.88		309.51
638.0	21.043	590.01	506.09	432.99	274.18	713.0	24.629		569.98		310.24
639.0	21.109	591.03	506.62	433.71	274.38	714.0	24.671		571.08		310.95
640.0	21.175	592.05	507.15	434.38	274.57	715.0	24.713		572.17		311.65
641.0	21.241	593.07	507.63	435.04	274.75	716.0	24.755		573.27		312.34
642.0	21.307	594.09	508.10	435.69	274.92	717.0	24.797		574.20		312.96
643.0	21.373	595.10	508.57	436.32	275.09	718.0	24.839		575.07		313.62
644.0	21.439	596.12	509.05	436.94	275.27	719.0	24.881		575.99		314.21
645.0	21.505	597.15	509.53	437.54	275.45	720.0	24.923		576.96		314.83
646.0	21.571	598.16	509.99	438.12	275.63	721.0	24.965		577.90		315.44
647.0	21.637	599.18	510.48	438.69	275.80	722.0	25.007		578.86		316.04
648.0	21.703	600.19	510.95	439.24	275.98	723.0	25.049		579.81		316.64
649.0	21.769	601.21	511.43	439.77	276.16	724.0	25.091		580.76		317.24
650.0	21.835	602.23	511.90	440.29	276.34	725.0	25.134		581.69		317.82
651.0	21.901	603.24	512.38	440.79	276.52	726.0	25.176		582.65		318.41
652.0	21.967	604.26	512.94	441.28	276.73	727.0	25.218		583.59		319.00
653.0	22.033	605.26	513.60	441.89	276.98	728.0	25.260		584.54		319.58
654.0	22.099	606.28	514.26	442.69	277.24	729.0	25.302		585.47		320.17
655.0	22.165	607.29	514.90	443.47	277.49	730.0	25.344		586.42		320.74
656.0	22.231	608.31	515.56	444.23	277.73	731.0	25.386		587.35		321.32
657.0	22.273	609.32	516.21	444.97	277.98	732.0	25.428		588.29		321.89
658.0	22.315	610.33	516.86	445.69	278.24	733.0	25.470		589.22		322.45
659.0	22.357	611.34	517.50	446.39	278.48	734.0	25.512		590.15		323.02
660.0	22.399	612.35	518.15	447.08	278.73	735.0	25.554		591.08		323.58
661.0	22.441	613.36	518.79	447.74	278.98	736.0	25.596		592.00		324.15
662.0	22.483	614.36	519.44	448.40	279.23	737.0	25.638		592.94		324.72
663.0	22.526	615.38	520.08	449.04	279.48	738.0	25.680		593.96		325.35

Note: Depths are based upon the well-log correlation between Hole 806B and Holes 586C, 807A, 805C, and 803D. The preliminary age scale is for Hole 806B. Correlation to Hole 803D is based upon the correlation between Holes 806B and 807A and between Holes 803D and 807A.

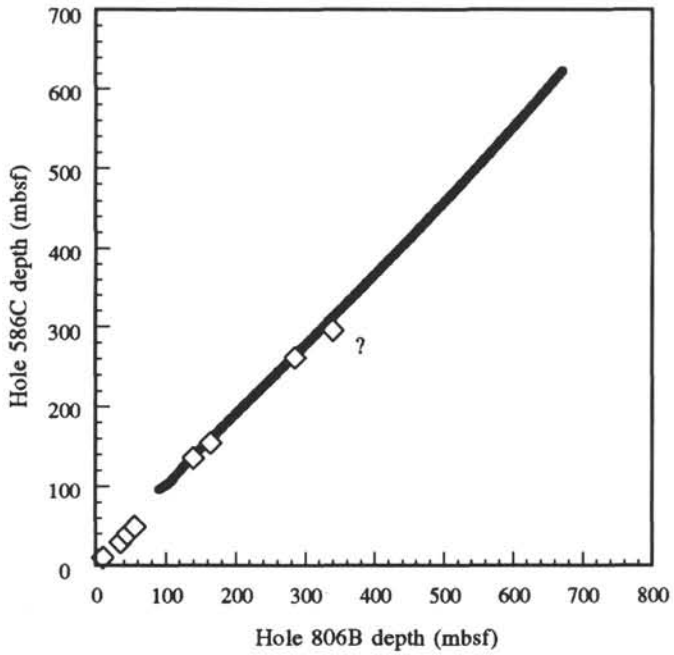

Figure 8. Stratigraphic correlation between Holes 806B and 586C, showing the inverse signal correlation map (solid line) compared to the nannofossil biostratigraphic events identified from the detailed post-cruise analysis (Takayama and Backman, this volume).

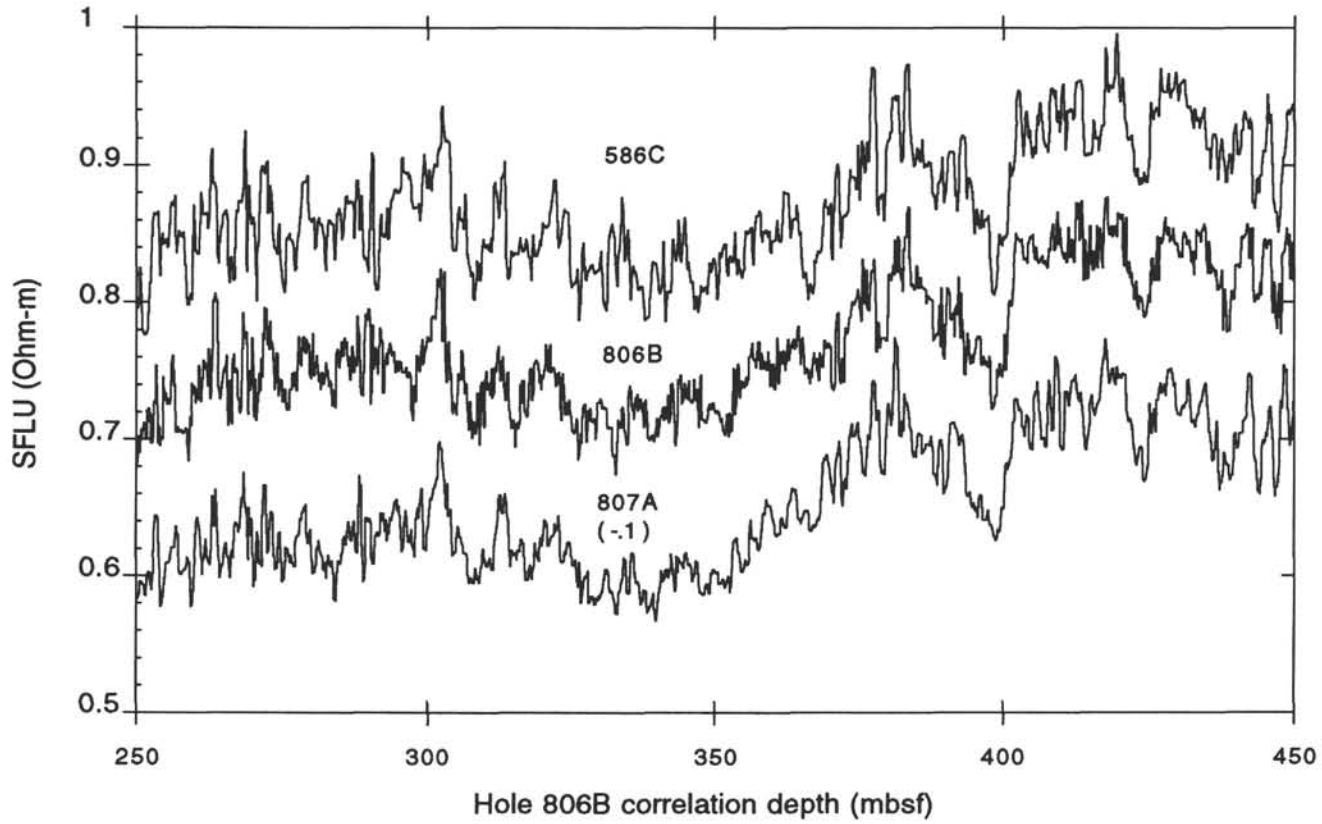

Figure 9. A section of the resistivity data from all the holes on top of the Ontong Java Plateau depth-shifted to the equivalent depth in Hole 806B. The records have been offset with respect to each other for clarity. Resistivity variations are probably a result of small-scale porosity changes between sedimentary beds that must have great lateral extent to be correlated between Holes 807A and 806B, almost 500 km apart.

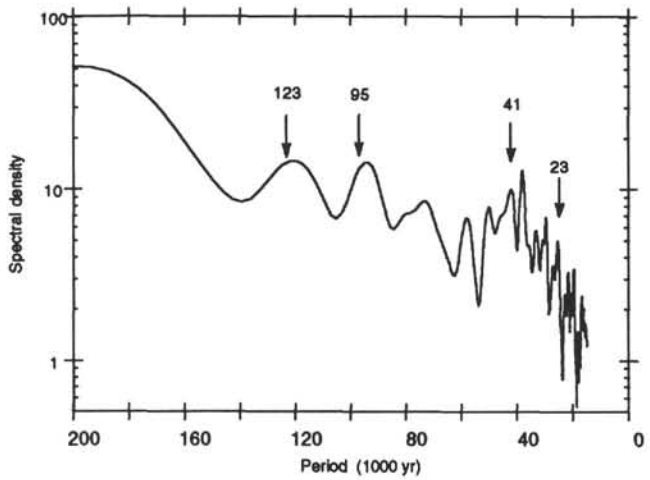

Figure 10. Spectral analysis of the SFLU section from 3.5 to 8.75 Ma in Hole 806B. The time scale is based on shipboard analyses. Split 41 and 23 k.y. periods point to the need for minor tuning of the sedimentation rates.

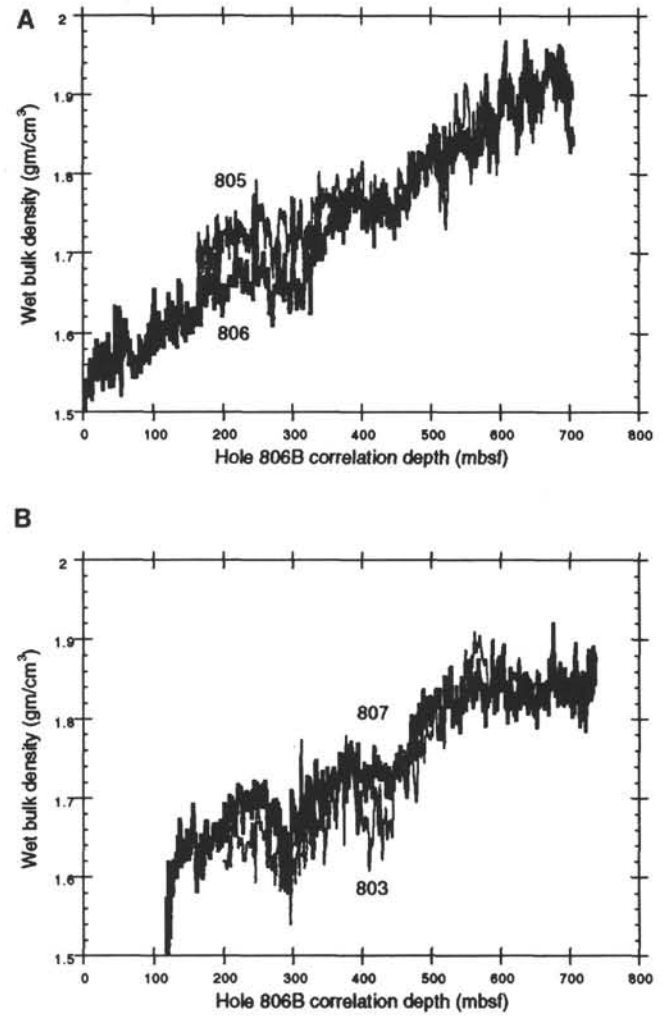

Figure 11. Correlation between Sites 806 and 805 (**A**) and Sites 807 and 803 (**B**). All depths are plotted on the reference Site 806 depth scale.

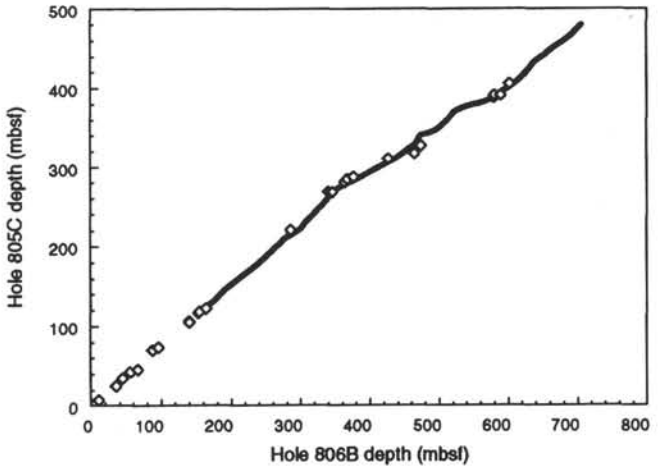

Figure 12. Stratigraphic correlation between Holes 806B and 805C, showing the inverse signal correlation map (solid line) compared to the nannofossil biostratigraphic events identified from the detailed post-cruise analysis (Takayama and Backman, this volume).

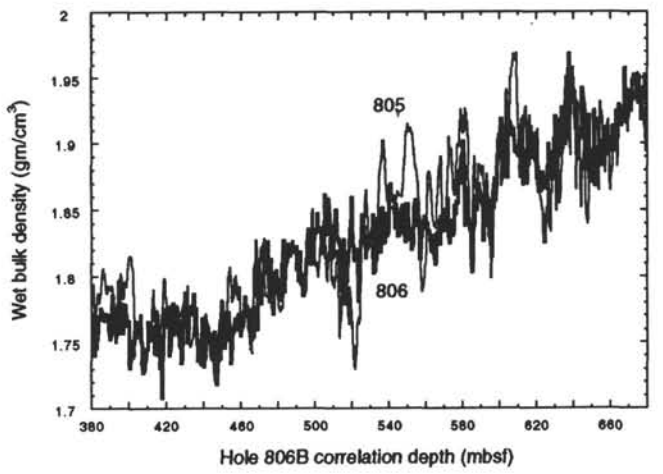

Figure 13. Detail of correlation between Holes 806B and 805C over the "kinky" interval in Figure 12.

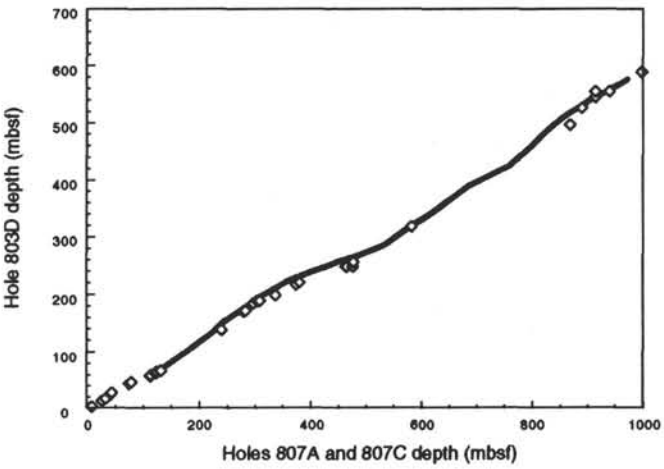

Figure 14. Stratigraphic correlation between Site 807 and Hole 803D, showing the inverse signal correlation map (solid line) compared to the nannofossil biostratigraphic events identified from the detailed post-cruise analysis (Takayama and Backman, this volume).

Table 2. Equivalent depths at Sites 803, 806, and 807 on the Ontong Java Plateau.

Hole 807A depth (mbsf)	Hole 807C depth (mbsf)	Site 807 age (Ma)	Hole 806B depth (mbsf)	Hole 803D depth (mbsf)	Hole 807A depth (mbsf)	Hole 807C depth (mbsf)	Site 807 age (Ma)	Hole 806B depth (mbsf)	Hole 803D depth (mbsf)	Hole 807A depth (mbsf)	Hole 807C depth (mbsf)	Site 807 age (Ma)	Hole 806B depth (mbsf)	Hole 803D depth (mbsf)
139.0		5.308	167.87	73.79	215.0		7.019	263.43	127.15	291.0		9.364	349.42	182.99
140.0		5.330	169.15	74.48	216.0		7.041	264.62	127.85	292.0		9.449	350.71	183.68
141.0		5.353	170.44	75.17	217.0		7.064	265.80	128.54	293.0		9.535	352.01	184.38
142.0		5.375	171.73	75.86	218.0		7.086	266.98	129.23	294.0		9.620	353.34	185.07
143.0		5.398	172.97	76.56	219.0		7.109	268.15	129.93	295.0		9.705	354.65	185.76
144.0		5.420	174.11	77.24	220.0		7.131	269.32	130.81	296.0		9.790	355.99	186.45
145.0		5.443	175.26	77.94	221.0		7.154	270.50	131.71	297.0		9.875	357.32	187.14
146.0		5.465	176.41	78.63	222.0		7.176	271.65	132.61	298.0		9.960	358.65	187.83
147.0		5.488	177.57	79.32	223.0		7.199	272.79	133.50	299.0		10.045	359.98	188.53
148.0		5.510	178.73	80.01	224.0		7.221	273.89	134.40	300.0		10.130	361.27	189.22
149.0		5.533	179.88	80.70	225.0		7.244	274.97	135.29	301.0		10.215	362.58	189.91
150.0		5.555	181.05	81.39	226.0		7.266	276.06	136.19	302.0		10.300	363.85	190.60
151.0		5.578	182.21	82.08	227.0		7.289	277.12	137.08	303.0		10.385	365.12	191.29
152.0		5.600	183.36	82.77	228.0		7.311	278.19	137.97	304.0		10.470	366.35	191.99
153.0		5.623	184.52	83.46	229.0		7.334	279.23	138.87	305.0		10.555	367.60	192.67
154.0		5.645	185.68	84.15	230.0		7.356	280.31	139.76	306.0		10.640	369.04	193.37
155.0		5.668	187.06	84.84	231.0		7.379	281.36	140.64	307.0		10.725	370.47	194.06
156.0		5.690	188.43	85.54	232.0		7.401	282.39	141.54	308.0		10.810	371.91	194.74
157.0		5.713	189.78	86.23	233.0		7.424	283.43	142.42	309.0		10.896	373.31	195.43
158.0		5.735	191.13	86.92	234.0		7.446	284.43	143.31	310.0		10.981	374.71	196.03
159.0		5.758	192.43	87.61	235.0		7.469	285.43	144.20	311.0		11.066	376.11	196.52
160.0		5.781	193.70	88.31	236.0		7.491	286.45	145.09	312.0		11.151	377.50	197.05
161.0		5.803	194.94	89.00	237.0		7.514	287.53	145.97	313.0		11.236	378.91	197.57
162.0		5.826	196.19	89.69	238.0		7.536	288.60	146.87	314.0		11.321	380.31	198.09
163.0		5.848	197.41	90.39	239.0		7.559	289.67	147.76	315.0		11.406	381.73	198.61
164.0		5.871	198.66	91.08	240.0		7.586	290.74	148.65	316.0		11.491	383.14	199.14
165.0		5.893	199.88	91.78	241.0		7.613	291.78	149.54	317.0		11.521	384.56	199.66
166.0		5.916	201.10	92.48	242.0		7.640	292.83	150.44	318.0		11.550	385.98	200.18
167.0		5.938	202.34	93.17	243.0		7.667	293.87	151.33	319.0		11.580	387.41	200.70
168.0		5.961	203.55	93.87	244.0		7.693	294.92	152.22	320.0		11.609	388.86	201.22
169.0		5.983	204.82	94.57	245.0		7.720	295.96	153.06	321.0		11.639	390.28	201.74
170.0		6.006	206.08	95.27	246.0		7.747	297.02	153.66	322.0		11.669	391.73	202.26
171.0		6.028	207.35	95.97	247.0		7.774	298.10	154.27	323.0		11.698	393.15	202.78
172.0		6.051	208.63	96.67	248.0		7.801	299.22	154.88	324.0		11.728	394.57	203.30
173.0		6.073	209.90	97.37	249.0		7.828	300.43	155.49	325.0		11.757	395.99	203.81
174.0		6.096	211.18	98.07	250.0		7.855	301.66	156.10	326.0		11.787	397.39	204.33
175.0		6.118	212.45	98.77	251.0		7.882	302.70	156.72	327.0		11.817	398.75	204.84
176.0		6.141	213.68	99.47	252.0		7.909	303.77	157.33	328.0		11.846	399.83	205.35
177.0		6.163	214.92	100.17	253.0		7.935	304.85	157.95	329.0		11.876	400.98	205.87
178.0		6.186	216.17	100.87	254.0		7.962	305.98	158.57	330.0		11.905	402.12	206.38
179.0		6.208	217.43	101.59	255.0		7.989	307.12	159.19	331.0		11.935	403.27	206.89
180.0		6.231	218.68	102.30	256.0		8.016	308.30	159.82	332.0		11.965	404.42	207.40
181.0		6.253	219.95	103.02	257.0		8.043	309.49	160.44	333.0		11.994	405.57	207.91
182.0		6.276	221.21	103.74	258.0		8.070	310.73	161.07	334.0		12.024	406.72	208.42
183.0		6.298	222.48	104.46	259.0		8.097	311.99	161.70	335.0		12.053	407.89	208.93
184.0		6.321	223.76	105.17	260.0		8.124	313.12	162.33	336.0		12.083	409.14	209.44
185.0		6.343	225.04	105.89	261.0		8.151	314.22	162.97	337.0		12.113	410.55	209.95
186.0		6.366	226.33	106.61	262.0		8.177	315.33	163.60	338.0		12.142	411.99	210.46
187.0		6.388	227.61	107.32	263.0		8.204	316.45	164.24	339.0		12.172	413.46	211.02
188.0		6.411	228.92	108.04	264.0		8.231	317.60	164.88	340.0		12.201	414.95	211.59
189.0		6.433	230.21	108.76	265.0		8.258	318.74	165.53	341.0		12.231	416.48	212.16
190.0		6.456	231.51	109.47	266.0		8.285	319.89	166.18	342.0		12.261	418.00	212.73
191.0		6.478	232.82	110.19	267.0		8.312	321.03	166.83	343.0		12.290	419.52	213.30
192.0		6.501	234.13	110.91	268.0		8.339	322.19	167.47	344.0		12.320	421.04	213.87
193.0		6.523	235.46	111.62	269.0		8.366	323.32	168.13	345.0		12.349	422.57	214.43
194.0		6.546	236.77	112.34	270.0		8.393	324.63	168.78	346.0		12.379	424.10	215.00
195.0		6.568	238.10	113.05	271.0		8.419	325.93	169.44	347.0		12.409	425.62	215.56
196.0		6.591	239.34	113.76	272.0		8.446	327.21	170.10	348.0		12.438	427.12	216.12
197.0		6.613	240.60	114.48	273.0		8.473	328.48	170.76	349.0		12.468	428.58	216.69
198.0		6.636	241.86	115.19	274.0		8.500	329.71	171.43	350.0		12.497	430.02	217.25
199.0		6.658	243.13	115.90	275.0		8.527	330.93	172.10	351.0		12.527	431.42	217.81
200.0		6.681	244.40	116.61	276.0		8.554	332.11	172.76	352.0		12.557	432.78	218.37
201.0		6.704	245.66	117.32	277.0		8.581	333.30	173.44	353.0		12.586	434.09	218.92
202.0		6.726	246.95	118.04	278.0		8.608	334.46	174.11	354.0		12.616	435.36	219.48
203.0		6.749	248.22	118.74	279.0		8.635	335.61	174.78	355.0		12.645	436.61	220.03
204.0		6.771	249.51	119.45	280.0		8.661	336.75	175.46	356.0		12.675	437.81	220.58
205.0		6.794	250.79	120.16	281.0		8.688	337.88	176.14	357.0	355.55	12.705	438.99	221.10
206.0		6.816	252.07	120.86	282.0		8.715	339.02	176.82	358.0	356.55	12.734	440.15	221.50
207.0		6.839	253.40	121.56	283.0		8.742	340.15	177.50	359.0	357.54	12.764	441.28	221.90
208.0		6.861	254.95	122.26	284.0		8.769	341.26	178.18	360.0	358.54	12.793	442.41	222.30
209.0		6.884	256.41	122.97	285.0		8.854	342.29	178.87	361.0	359.54	12.823	443.52	222.70
210.0		6.906	257.56	123.67	286.0		8.939	343.33	179.55	362.0	360.55	12.853	444.64	223.10
211.0		6.929	258.73	124.37	287.0		9.024	344.41	180.24	363.0	361.57	12.882	445.76	223.50
212.0		6.951	259.89	125.07	288.0		9.109	345.63	180.92	364.0	362.60	12.912	446.89	223.89
213.0		6.974	261.06	125.76	289.0		9.194	346.88	181.61	365.0	363.63	12.941	448.11	224.29
214.0		6.996	262.25	126.46	290.0		9.279	348.14	182.30	366.0	364.68	12.971	449.36	224.68

Table 2 (continued).

Hole 807A depth (mbsf)	Hole 807C depth (mbsf)	Site 807 age (Ma)	Hole 806B depth (mbsf)	Hole 803D depth (mbsf)	Hole 807A depth (mbsf)	Hole 807C depth (mbsf)	Site 807 age (Ma)	Hole 806B depth (mbsf)	Hole 803D depth (mbsf)	Hole 807A depth (mbsf)	Hole 807C depth (mbsf)	Site 807 age (Ma)	Hole 806B depth (mbsf)	Hole 803D depth (mbsf)
367.0	365.73	13.001	450.67	225.07	442.0	440.86	17.293	554.22	252.73	517.0	516.47	21.680	658.21	278.29
368.0	366.79	13.030	451.99	225.46	443.0	441.90	17.366	555.67	253.12	518.0	517.47	21.721	659.76	278.67
369.0	367.86	13.060	453.36	225.85	444.0	442.93	17.439	557.13	253.59	519.0	518.47	21.761	661.31	279.06
370.0	368.94	13.089	454.77	226.24	445.0	443.98	17.512	558.57	254.06	520.0	519.48	21.801	662.88	279.45
371.0	370.02	13.119	456.23	226.62	446.0	445.03	17.584	559.99	254.53	521.0	520.48	21.842	664.18	279.85
372.0	371.10	13.149	457.74	227.01	447.0	446.08	17.657	561.40	255.01	522.0	521.48	21.882	665.34	280.24
373.0	372.18	13.178	459.27	227.39	448.0	447.13	17.730	562.82	255.48	523.0	522.48	21.922	666.50	280.64
374.0	373.26	13.208	460.85	227.78	449.0	448.18	17.803	564.25	255.95	524.0	523.48	21.963	667.66	281.04
375.0	374.34	13.237	462.44	228.15	450.0	449.23	17.875	565.57	256.33	525.0	524.49	22.003	668.83	281.44
376.0	375.41	13.267	464.04	228.54	451.0	450.28	17.948	566.84	256.59	526.0	525.49	22.043	669.99	281.85
377.0	376.47	13.297	465.55	228.91	452.0	451.33	18.021	568.11	256.87	527.0	526.49	22.084	671.17	282.25
378.0	377.53	13.326	466.99	229.29	453.0	452.37	18.094	569.38	257.16	528.0	527.49	22.124	672.18	282.66
379.0	378.57	13.356	468.40	229.67	454.0	453.41	18.167	570.66	257.44	529.0	528.50	22.164	673.07	283.07
380.0	379.60	13.385	469.77	230.04	455.0	454.45	18.239	572.18	257.72	530.0	529.50	22.205	673.95	283.48
381.0	380.62	13.415	471.11	230.41	456.0	455.48	18.312	574.09	258.01	531.0	530.50	22.245	674.86	283.90
382.0	381.63	13.445	472.39	230.79	457.0	456.51	18.385	576.00	258.29	532.0	531.49	22.285	675.74	284.30
383.0	382.63	13.474	473.66	231.16	458.0	457.53	18.458	577.93	258.58	533.0	532.49	22.326	676.70	284.98
384.0	383.61	13.504	474.88	231.53	459.0	458.55	18.530	579.83	258.86	534.0	533.48	22.366	677.69	285.66
385.0	384.59	13.533	476.10	231.89	460.0	459.57	18.603	581.75	259.14	535.0	534.48	22.406	678.68	286.34
386.0	385.55	13.563	477.29	232.26	461.0	460.58	18.676	583.67	259.42	536.0	535.47	22.446	679.67	287.03
387.0	386.51	13.593	478.46	232.63	462.0	461.59	18.749	585.23	259.71	537.0	536.46	22.487	680.65	287.72
388.0	387.47	13.622	479.58	232.99	463.0	462.59	18.822	586.22	259.99	538.0	537.44	22.527	681.63	288.40
389.0	388.42	13.652	480.54	233.35	464.0	463.60	18.894	587.20	260.27	539.0	538.43	22.567	682.62	289.09
390.0	389.36	13.681	481.51	233.72	465.0	464.59	18.967	588.17	260.55	540.0	539.41	22.608	683.60	289.79
391.0	390.31	13.711	482.48	234.08	466.0	465.59	19.040	589.16	260.83	541.0	540.39	22.648	684.59	290.48
392.0	391.26	13.741	483.47	234.44	467.0	466.58	19.113	590.13	261.11	542.0	541.37	22.688	685.56	291.17
393.0	392.21	13.770	484.48	234.80	468.0	467.57	19.185	591.12	261.39	543.0	542.35	22.729	686.57	291.87
394.0	393.17	13.800	485.49	235.16	469.0	468.56	19.258	592.09	261.67	544.0	543.33	22.769	687.62	292.56
395.0	394.13	13.873	486.54	235.52	470.0	469.55	19.331	593.07	261.95	545.0	544.30	22.809	688.66	293.26
396.0	395.10	13.945	487.60	235.87	471.0	470.53	19.404	594.06	262.22	546.0	545.28	22.850	689.72	293.95
397.0	396.08	14.018	488.70	236.23	472.0	471.52	19.477	595.03	262.50	547.0	546.26	22.890	690.75	294.65
398.0	397.07	14.091	489.83	236.59	473.0	472.50	19.549	596.02	262.77	548.0	547.24	22.930	691.80	295.35
399.0	398.08	14.164	491.00	236.94	474.0	473.48	19.622	596.99	263.05	549.0	548.22	22.971	692.83	296.04
400.0	399.09	14.237	492.35	237.30	475.0	474.46	19.695	597.98	263.32	550.0	549.21	23.011	693.88	296.74
401.0	400.11	14.309	493.83	237.65	476.0	475.44	19.768	598.95	263.60	551.0	550.19	23.051	694.90	297.43
402.0	401.15	14.382	495.37	238.01	477.0	476.43	19.840	600.22	263.87	552.0	551.17	23.092	695.93	298.13
403.0	402.20	14.455	496.93	238.36	478.0	477.41	19.913	601.69	264.14	553.0	552.16	23.132	696.95	298.82
404.0	403.25	14.528	498.53	238.72	479.0	478.39	19.986	603.15	264.43	554.0	553.15	23.172	698.13	299.51
405.0	404.31	14.600	499.88	239.07	480.0	479.38	20.059	604.62	264.79	555.0	554.14	23.213	699.33	300.20
406.0	405.38	14.673	501.16	239.43	481.0	480.36	20.132	606.08	265.15	556.0	555.14	23.253	700.38	300.89
407.0	406.45	14.746	502.46	239.78	482.0	481.35	20.204	607.46	265.51	557.0	556.13	23.293	701.29	301.57
408.0	407.53	14.819	503.76	240.14	483.0	482.33	20.277	608.76	265.87	558.0	557.13	23.334	702.20	302.25
409.0	408.60	14.892	505.11	240.49	484.0	483.32	20.350	610.09	266.23	559.0	558.12	23.374	703.09	302.93
410.0	409.67	14.964	506.57	240.85	485.0	484.31	20.390	611.40	266.59	560.0	559.12	23.414	704.00	303.61
411.0	410.73	15.037	508.56	241.20	486.0	485.30	20.430	612.70	266.95	561.0	560.11	23.454	704.89	304.29
412.0	411.79	15.110	510.54	241.56	487.0	486.30	20.471	614.01	267.31	562.0	561.11	23.495	705.80	304.96
413.0	412.83	15.183	512.51	241.92	488.0	487.29	20.511	615.29	267.66	563.0	562.10	23.535	706.70	305.64
414.0	413.87	15.255	514.49	242.27	489.0	488.29	20.551	616.59	268.02	564.0	563.09	23.575	707.60	306.30
415.0	414.89	15.328	516.45	242.64	490.0	489.29	20.592	617.86	268.38	565.0	564.09	23.616	708.50	306.97
416.0	415.90	15.401	518.42	242.99	491.0	490.29	20.632	619.14	268.74	566.0	565.08	23.656	709.40	307.63
417.0	416.90	15.474	520.37	243.35	492.0	491.29	20.672	620.41	269.09	567.0	566.06	23.696	710.31	308.29
418.0	417.89	15.547	522.16	243.71	493.0	492.30	20.713	621.66	269.45	568.0	567.05	23.737	711.21	308.95
419.0	418.86	15.619	523.43	244.08	494.0	493.31	20.753	622.91	269.81	569.0	568.03	23.777	712.12	309.60
420.0	419.82	15.692	524.67	244.44	495.0	494.32	20.793	624.14	270.17	570.0	569.01	23.817	713.02	310.25
421.0	420.78	15.765	525.91	244.80	496.0	495.33	20.834	625.37	270.52	571.0	569.99	23.858	713.93	310.90
422.0	421.72	15.838	527.15	245.17	497.0	496.34	20.874	626.59	270.88	572.0	570.97	23.898	714.84	311.54
423.0	422.66	15.910	528.40	245.53	498.0	497.35	20.914	627.80	271.24	573.0	571.94	23.938	715.75	312.18
424.0	423.59	15.983	529.65	245.90	499.0	498.36	20.955	629.00	271.60	574.0	572.92	23.979	716.78	312.82
425.0	424.52	16.056	530.91	246.27	500.0	499.38	20.995	630.20	271.96	575.0	573.89	24.019	717.92	313.57
426.0	425.44	16.129	532.15	246.64	501.0	500.39	21.035	631.39	272.32	576.0	574.86	24.059	719.01	314.22
427.0	426.36	16.202	533.41	247.01	502.0	501.40	21.076	632.55	272.68	577.0	575.83	24.100	720.05	314.86
428.0	427.28	16.274	534.66	247.38	503.0	502.42	21.116	633.72	273.05	578.0	576.81	24.140	721.10	315.50
429.0	428.21	16.347	535.92	247.76	504.0	503.43	21.156	634.89	273.41	579.0	577.78	24.180	722.15	316.13
430.0	429.14	16.420	537.28	248.13	505.0	504.44	21.197	636.04	273.78	580.0	578.75	24.221	723.20	316.76
431.0	430.07	16.493	538.66	248.51	506.0	505.45	21.237	637.82	274.15	581.0	579.73	24.261	724.26	317.39
432.0	431.01	16.565	540.04	248.89	507.0	506.45	21.277	639.71	274.52	582.0	580.71	24.301	725.32	318.01
433.0	431.95	16.638	541.44	249.26	508.0	507.46	21.318	641.79	274.88	583.0	581.69	24.342	726.37	318.63
434.0	432.91	16.711	542.83	249.64	509.0	508.46	21.358	643.89	275.25	584.0	582.67	24.382	727.43	319.25
435.0	433.87	16.784	544.24	250.02	510.0	509.47	21.398	646.01	275.63	585.0	583.66	24.422	728.49	319.87
436.0	434.84	16.857	545.64	250.41	511.0	510.47	21.438	648.10	276.00	586.0	584.65	24.462	729.56	320.49
437.0	435.82	16.929	547.05	250.79	512.0	511.47	21.479	650.20	276.38	587.0	585.64	24.503	730.62	321.10
438.0	436.81	17.002	548.48	251.18	513.0	512.47	21.519	652.09	276.75	588.0	586.63	24.543	731.69	321.71
439.0	437.81	17.075	549.89	251.56	514.0	513.47	21.559	653.61	277.14	589.0	587.63	24.583	732.77	322.32
440.0	438.82	17.148	551.34	251.95	515.0	514.47	21.600	655.14	277.52	590.0	588.62	24.624	733.84	322.93
441.0	439.84	17.220	552.77	252.34	516.0	515.47	21.640	656.67	277.90	591.0	589.63	24.664	734.92	323.54

Table 2 (continued).

Hole 807A depth (mbsf)	Hole 807C depth (mbsf)	Site 807 age (Ma)	Hole 806B depth (mbsf)	Hole 803D depth (mbsf)	Hole 807A depth (mbsf)	Hole 807C depth (mbsf)	Site 807 age (Ma)	Hole 806B depth (mbsf)	Hole 803D depth (mbsf)	Hole 807A depth (mbsf)	Hole 807C depth (mbsf)	Site 807 age (Ma)	Hole 806B depth (mbsf)	Hole 803D depth (mbsf)
592.0	590.63	24.704	736.00	324.15	667.0	667.22	27.728		375.80	742.0	741.69	30.752		415.72
593.0	591.63	24.745	737.07	324.76	668.0	668.18	27.769		376.52	743.0	742.68	30.793		416.18
594.0	592.64	24.785	738.03	325.37	669.0	669.14	27.809		377.23	744.0	743.67	30.833		416.65
595.0	593.64	24.825		325.97	670.0	670.10	27.849		377.96	745.0	744.67	30.873		417.12
596.0	594.64	24.866		326.58	671.0	671.07	27.890		378.68	746.0	745.67	30.914		417.58
597.0	595.64	24.906		327.18	672.0	672.04	27.930		379.39	747.0	746.66	30.954		418.05
598.0	596.64	24.946		327.79	673.0	673.02	27.970		380.11	748.0	747.67	30.994		418.51
599.0	597.64	24.987		328.39	674.0	674.01	28.011		380.83	749.0	748.67	31.035		418.97
600.0	598.64	25.027		329.00	675.0	674.99	28.051		381.55	750.0	749.67	31.075		419.43
601.0	599.64	25.067		329.60	676.0	675.99	28.091		382.27	751.0	750.68	31.115		419.88
602.0	600.63	25.108		330.21	677.0	676.98	28.132		382.99	752.0	751.68	31.156		420.34
603.0	601.62	25.148		330.82	678.0	677.98	28.172		383.71	753.0	752.69	31.196		420.79
604.0	602.60	25.188		331.42	679.0	678.99	28.212		384.43	754.0	753.70	31.236		421.24
605.0	603.59	25.229		332.03	680.0	680.00	28.253		385.16	755.0	754.70	31.277		421.70
606.0	604.57	25.269		332.63	681.0	681.01	28.293		385.88	756.0	755.71	31.317		422.15
607.0	605.55	25.309		333.24	682.0	682.03	28.333		386.61	757.0	756.71	31.357		422.68
608.0	606.53	25.350		333.85	683.0	683.04	28.374		387.33	758.0	757.72	31.398		423.35
609.0	607.50	25.390		334.46	684.0	684.06	28.414		388.06	759.0	758.72	31.438		424.22
610.0	608.48	25.430		335.08	685.0	685.07	28.454		388.80	760.0	759.72	31.478		425.10
611.0	609.45	25.470		335.69	686.0	686.09	28.495		389.32	761.0	760.72	31.519		425.98
612.0	610.43	25.511		336.31	687.0	687.10	28.535		389.77	762.0	761.72	31.559		426.85
613.0	611.40	25.551		336.92	688.0	688.11	28.575		390.22	763.0	762.72	31.599		427.72
614.0	612.38	25.591		337.54	689.0	689.12	28.615		390.67	764.0	763.71	31.639		428.60
615.0	613.35	25.632		338.15	690.0	690.13	28.656		391.11	765.0	764.71	31.680		429.47
616.0	614.34	25.672		338.77	691.0	691.13	28.696		391.56	766.0	765.70	31.720		430.34
617.0	615.32	25.712		339.39	692.0	692.13	28.736		392.01	767.0	766.70	31.760		431.21
618.0	616.30	25.753		340.01	693.0	693.12	28.777		392.46	768.0	767.70	31.801		432.08
619.0	617.29	25.793		340.63	694.0	694.11	28.817		392.92	769.0	768.69	31.841		432.95
620.0	618.27	25.833		341.26	695.0	695.10	28.857		393.37	770.0	769.68	31.881		433.81
621.0	619.25	25.874		341.98	696.0	696.08	28.898		393.83	771.0	770.68	31.922		434.68
622.0	620.23	25.914		342.72	697.0	697.07	28.938		394.29	772.0	771.68	31.962		435.55
623.0	621.22	25.954		343.45	698.0	698.05	28.978		394.74	773.0	772.67	32.002		436.42
624.0	622.21	25.995		344.18	699.0	699.02	29.019		395.20	774.0	773.67	32.043		437.29
625.0	623.21	26.035		344.92	700.0	700.00	29.059		395.66	775.0	774.67	32.083		438.16
626.0	624.21	26.075		345.65	701.0	700.98	29.099		396.12	776.0	775.67	32.123		439.04
627.0	625.22	26.116		346.39	702.0	701.95	29.140		396.59	777.0	776.67	32.164		439.92
628.0	626.24	26.156		347.13	703.0	702.93	29.180		397.06	778.0	777.67	32.204		440.79
629.0	627.22	26.196		347.87	704.0	703.91	29.220		397.52	779.0	778.67	32.244		441.67
630.0	628.19	26.237		348.61	705.0	704.89	29.261		397.99	780.0	779.67	32.285		442.55
631.0	629.16	26.277		349.35	706.0	705.87	29.301		398.46	781.0	780.68	32.325		443.43
632.0	630.14	26.317		350.09	707.0	706.85	29.341		398.93	782.0	781.68	32.365		444.32
633.0	631.12	26.358		350.83	708.0	707.84	29.382		399.40	783.0	782.68	32.406		445.20
634.0	632.11	26.398		351.57	709.0	708.83	29.422		399.88	784.0	783.69	32.446		446.10
635.0	633.10	26.438		352.32	710.0	709.83	29.462		400.36	785.0	784.69	32.486		446.99
636.0	634.09	26.479		353.06	711.0	710.82	29.503		400.83	786.0	785.69	32.527		447.89
637.0	635.09	26.519		353.80	712.0	711.82	29.543		401.31	787.0	786.69	32.567		448.79
638.0	636.09	26.559		354.54	713.0	712.82	29.583		401.79	788.0	787.69	32.607		449.70
639.0	637.10	26.599		355.29	714.0	713.83	29.623		402.27	789.0	788.69	32.647		450.61
640.0	638.12	26.640		356.03	715.0	714.84	29.664		402.75	790.0	789.69	32.688		451.52
641.0	639.13	26.680		356.77	716.0	715.84	29.704		403.23	791.0	790.69	32.728		452.44
642.0	640.14	26.720		357.52	717.0	716.85	29.744		403.71	792.0	791.68	32.768		453.35
643.0	641.15	26.761		358.26	718.0	717.86	29.785		404.19	793.0	792.68	32.809		454.27
644.0	642.16	26.801		359.00	719.0	718.87	29.825		404.68	794.0	793.67	32.849		455.19
645.0	643.16	26.841		359.73	720.0	719.88	29.865		405.16	795.0	794.67	32.889		456.12
646.0	644.16	26.882		360.48	721.0	720.89	29.906		405.64	796.0	795.66	32.930		457.05
647.0	645.34	26.922		361.22	722.0	721.89	29.946		406.13	797.0	796.66	32.970		457.99
648.0	646.56	26.962		361.96	723.0	722.90	29.986		406.62	798.0	797.65	33.010		458.93
649.0	647.77	27.003		362.69	724.0	723.90	30.027		407.10	799.0	798.65	33.051		459.86
650.0	648.96	27.043		363.43	725.0	724.90	30.067		407.58	800.0	799.64	33.091		460.81
651.0	650.15	27.083		364.17	726.0	725.90	30.107		408.07	801.0	800.64	33.131		461.75
652.0	651.33	27.124		364.90	727.0	726.89	30.148		408.55	802.0	801.64	33.172		462.69
653.0	652.50	27.164		365.63	728.0	727.89	30.188		409.03	803.0	802.64	33.212		463.64
654.0	653.66	27.204		366.37	729.0	728.88	30.228		409.52	804.0	803.65	33.252		464.58
655.0	654.81	27.245		367.10	730.0	729.87	30.269		410.00	805.0	804.65	33.293		465.54
656.0	655.95	27.285		367.83	731.0	730.85	30.309		410.48	806.0	805.66	33.333		466.49
657.0	657.09	27.325		368.56	732.0	731.84	30.349		410.96	807.0	806.68	33.373		467.43
658.0	658.22	27.366		369.29	733.0	732.82	30.390		411.44	808.0	807.70	33.414		468.38
659.0	659.34	27.406		370.02	734.0	733.81	30.430		411.92	809.0	808.72	33.454		469.34
660.0	660.46	27.446		370.74	735.0	734.79	30.470		412.40	810.0	809.74	33.494		470.29
661.0	661.47	27.487		371.47	736.0	735.77	30.511		412.88	811.0	810.77	33.535		471.23
662.0	662.43	27.527		372.19	737.0	736.76	30.551		413.35	812.0	811.80	33.575		472.18
663.0	663.39	27.567		372.91	738.0	737.74	30.591		413.83	813.0	812.84	33.615		473.13
664.0	664.35	27.607		373.64	739.0	738.73	30.631		414.30	814.0	813.88	33.655		474.07
665.0	665.30	27.648		374.36	740.0	739.71	30.672		414.78	815.0	814.92	33.696		475.01
666.0	666.26	27.688		375.08	741.0	740.70	30.712		415.25	816.0	815.96	33.736		475.95

Table 2 (continued).

Hole 807A	Hole 807C	Site 807	Hole 806B	Hole 803D	Hole 807A	Hole 807C	Site 807	Hole 806B	Hole 803D	Hole 807A	Hole 807C	Site 807	Hole 806B	Hole 803D
depth (mbsf)	depth (mbsf)	age (Ma)	depth (mbsf)	depth (mbsf)	depth (mbsf)	depth (mbsf)	age (Ma)	depth (mbsf)	depth (mbsf)	depth (mbsf)	depth (mbsf)	age (Ma)	depth (mbsf)	depth (mbsf)
817.0	817.00	33.776		476.88		879.00	36.276		523.41		941.00	38.776		557.93
818.0	818.05	33.817		477.81		880.00	36.317		524.01		942.00	38.816		558.46
	819.00	33.857		478.73		881.00	36.357		524.60		943.00	38.857		558.99
	820.00	33.897		479.66		882.00	36.397		525.20		944.00	38.897		559.53
	821.00	33.938		480.58		883.00	36.438		525.80		945.00	38.937		560.07
	822.00	33.978		481.49		884.00	36.478		526.40		946.00	38.978		560.60
	823.00	34.018		482.39		885.00	36.518		527.01		947.00	39.018		561.14
	824.00	34.059		483.30		886.00	36.559		527.61		948.00	39.058		561.68
	825.00	34.099		484.19		887.00	36.599		528.22		949.00	39.099		562.23
	826.00	34.139		485.08		888.00	36.639		528.83		950.00	39.139		562.77
	827.00	34.180		485.96		889.00	36.680		529.44		951.00	39.179		563.32
	828.00	34.220		486.85		890.00	36.720		530.06		952.00	39.220		563.87
	829.00	34.260		487.72		891.00	36.760		530.68		953.00	39.260		564.42
	830.00	34.301		488.58		892.00	36.800		531.30		954.00	39.300		564.98
	831.00	34.341		489.43		893.00	36.841		531.92		955.00	39.341		565.53
	832.00	34.381		490.28		894.00	36.881		532.55		956.00	39.381		566.09
	833.00	34.422		491.13		895.00	36.921		533.18		957.00	39.421		566.66
	834.00	34.462		491.97		896.00	36.962		533.82		958.00	39.462		567.23
	835.00	34.502		492.79		897.00	37.002		534.45		959.00	39.502		567.80
	836.00	34.543		493.62		898.00	37.042		535.09		960.00	39.542		568.37
	837.00	34.583		494.44		899.00	37.083		535.73		961.00	39.583		568.95
	838.00	34.623		495.24		900.00	37.123		536.37		962.00	39.623		569.54
	839.00	34.663		496.04		901.00	37.163		537.02		963.00	39.663		570.12
	840.00	34.704		496.83		902.00	37.204		537.61		964.00	39.704		570.72
	841.00	34.744		497.63		903.00	37.244		538.09		965.00	39.744		571.32
	842.00	34.784		498.41		904.00	37.284		538.59		966.00	39.784		571.91
	843.00	34.825		499.18		905.00	37.325		539.09		967.00	39.824		572.52
	844.00	34.865		499.96		906.00	37.365		539.60		968.00	39.865		573.13
	845.00	34.905		500.77		907.00	37.405		540.10		969.00	39.905		573.75
	846.00	34.946		501.56		908.00	37.446		540.61		970.00	39.945		574.38
	847.00	34.986		502.36		909.00	37.486		541.13		971.00	39.986		575.00
	848.00	35.026		503.15		910.00	37.526		541.64		972.00	40.026		575.64
	849.00	35.067		503.93		911.00	37.567		542.15		973.00	40.066		576.27
	850.00	35.107		504.71		912.00	37.607		542.67		974.00	40.107		576.91
	851.00	35.147		505.48		913.00	37.647		543.19		975.00	40.147		577.57
	852.00	35.188		506.24		914.00	37.688		543.70		976.00	40.187		578.22
	853.00	35.228		507.00		915.00	37.728		544.22		977.00	40.228		578.88
	854.00	35.268		507.76		916.00	37.768		544.74		978.00	40.268		579.54
	855.00	35.309		508.51		917.00	37.808		545.27		979.00	40.308		580.21
	856.00	35.349		509.26		918.00	37.849		545.79		980.00	40.349		580.89
	857.00	35.389		510.00		919.00	37.889		546.31		981.00	40.389		581.56
	858.00	35.430		510.73		920.00	37.929		546.84		982.00	40.429		582.25
	859.00	35.470		511.47		921.00	37.970		547.36		983.00	40.470		582.94
	860.00	35.510		512.16		922.00	38.010		547.89		984.00	40.510		583.63
	861.00	35.551		512.76		923.00	38.050		548.41		985.00	40.550		584.33
	862.00	35.591		513.36		924.00	38.091		548.94		986.00	40.591		585.04
	863.00	35.631		513.95		925.00	38.131		549.47		987.00	40.631		585.74
	864.00	35.671		514.55		926.00	38.171		549.99		988.00	40.671		586.46
	865.00	35.712		515.14		927.00	38.212		550.52		989.00	40.712		587.17
	866.00	35.752		515.74		928.00	38.252		551.05		990.00	40.752		587.89
	867.00	35.792		516.33		929.00	38.292		551.57		991.00	40.792		588.78
	868.00	35.833		516.92		930.00	38.333		552.10		992.00	40.832		589.86
	869.00	35.873		517.51		931.00	38.373		552.63		993.00	40.873		590.94
	870.00	35.913		518.10		932.00	38.413		553.16		994.00	40.913		592.01
	871.00	35.954		518.69		933.00	38.454		553.69		995.00	40.953		593.10
	872.00	35.994		519.28		934.00	38.494		554.22		996.00	40.994		594.18
	873.00	36.034		519.87		935.00	38.534		554.74		997.00	41.034		595.45
	874.00	36.075		520.45		936.00	38.575		555.28		998.00	41.074		596.74
	875.00	36.115		521.05		937.00	38.615		555.80		999.00	41.115		598.03
	876.00	36.155		521.64		938.00	38.655		556.34		1000.00	41.155		599.33
	877.00	36.196		522.23		939.00	38.696		556.86					
	878.00	36.236		522.82		940.00	38.736		557.39					

Note: Equivalent depths are based upon the well-log correlation between Holes 807A and 807C and Holes 806B and 803D. Age scale is from Site 807 and is preliminary.

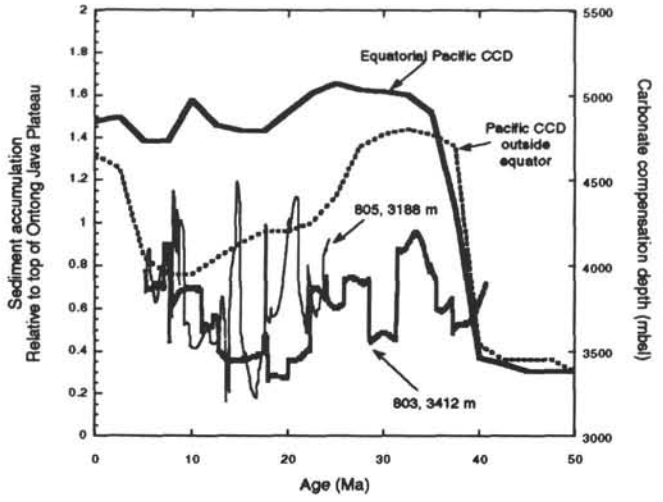

Figure 15. Sediment accumulation down the flank of the Ontong Java Plateau relative to drill sites on the top of the plateau. Also shown are previous estimates of the Pacific CCD from DSDP drilling (van Andel and Moore, 1974; van Andel et al., 1975). The CCD data were inverted so that sediment accumulation and CCD changes should have the same sense of direction. The deepest Ontong Java Plateau site logged, Hole 803D, shows an accumulation pattern vaguely resembling the equatorial CCD, but the intermediate site, Hole 805, alternates between accumulating sediments at the same rate as the top of the plateau and Hole 803D.

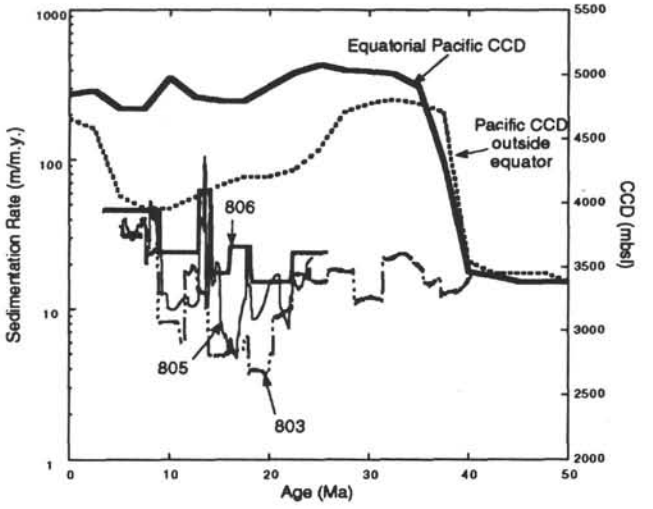

Figure 16. Sedimentation rates of three Ontong Java Plateau sites that form a transect down the flank of the plateau. Sedimentation rates, a crude measure of carbonate accumulation, show no resemblance to the earlier CCD information. Sedimentation on the flanks of the Ontong Java Plateau does not appear to have been controlled by depth-dependent carbonate dissolution.